THE UNIVERSITY
of EDINBURGH

This thesis has been submitted in fulfilment of the requirements for a postgraduate degree (e.g. PhD, MPhil, DClinPsychol) at the University of Edinburgh. Please note the following terms and conditions of use:

This work is protected by copyright and other intellectual property rights, which are retained by the thesis author, unless otherwise stated.
A copy can be downloaded for personal non-commercial research or study, without prior permission or charge.
This thesis cannot be reproduced or quoted extensively from without first obtaining permission in writing from the author.
The content must not be changed in any way or sold commercially in any format or medium without the formal permission of the author.
When referring to this work, full bibliographic details including the author, title, awarding institution and date of the thesis must be given.

The Functional Role of Vangl2 in Bile Duct Injury

David H.L. Wilson

A thesis submitted for the degree of MSc by Research at The University of Edinburgh

2017

Declaration

I confirm that this thesis presented for the degree of Masters in Science by Research has been composed entirely by myself, is solely the result of my own work and has not been submitted for any other degree or professional qualification

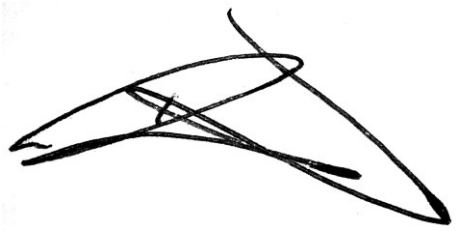

9th May 2017

David H.L. Wilson

Abstract

The Liver is comprised of hepatocytes, the parenchymal cells, and non-parenchymal cells which includes stellate cells, portal fibroblasts, inflammatory cells and cholangiocytes. Cholangiocytes are the epithelial cells of the bile ducts, which carry bile from the liver to the duodenum. Bile ducts and specifically cholangiocytes are susceptible to disease; these diseases are classified as cholangiopathies. Primary Sclerosing Cholangitis (PSC) is a disease of both the extra- and intrahepatic bile ducts involving inflammation and obliterative fibrosis. The cause of PSC is, as yet unclear, but is thought to be autoimmune related. Inflammation of tissue surrounding the ducts leads to stricture and sclerosing of the duct and results in scar formation, thereby, leading to obstruction of bile flow. Chronic impairment of the duct accompanied by dysfunction of bile transport results in biliary fibrosis, progressive biliary cirrhosis and liver failure. PSC is increasing in prevalence, untreatable and, ultimately, requires transplantation. Given donor liver numbers have remained static over the last 30 years, modulating fibrosis is an attractive alternative to transplantation. Tissue fibrosis is a complex process involving the formation of an excess of fibrous tissue. Fibrosis is an important part of the regenerative process during injury. It requires balanced expression of fibrotic promotors (e.g. Transforming Growth Factor β (TGFβ) and Matrix Metalloproteinases (MMPs)) and inhibitors (e.g. Tissue Inhibitor of Metalloproteinases (TIMPs)) to maintain an environment conducive to tissue repair and continued organ function.

The non-canonical Wnt signaling pathway has been, traditionally, shown to determine cellular polarity and cell migration during embryogenesis, however, its role in adult tissue homeostasis and regeneration is poorly understood. Examples of non-canonical Wnt pathway activation have been described during regeneration, for example, in skeletal

muscle, however the role of non-canonical Wnt signaling in the liver has not been elucidated. Briefly, the non-canonical Wnt pathway does not involve β-catenin, unlike the canonical pathway or calcium, as in the calcium mediated Wnt Pathway. Wnt ligand binds to a Frizzled (Fzd) receptor or a single pass receptor tyrosine-kinase (such as Ror2 or Ptk7) which can then interact with the co-receptor Van Gogh-like 2 (Vangl2). Activation of this receptor recruits Disheveled (Dsh) to the cell membrane. Downstream of Dsh the pathway can utilise a number of signaling cascades involving activation of DAAM1, Rho, Rac, ROCK and Jnk that ultimately leads to actin cytoskeletal modifications and/or transcription via AP-1. Inhibition of these key downstream components has been shown to phenocopy knockout of the cell surface receptor elements demonstrating the specific nature of the pathway to its desired biological effect. Here we use a mouse model of PSC to show up-regulation of the non-canonical Wnt pathway receptor-ligand complex and downstream activation of the Vangl2 mediated non-canonical Wnt pathway. Particularly, we show that Vangl2 and Wnt5a are up regulated at both the transcript and protein level and also demonstrate that these proteins are expressed in the regenerating ducts following PSC-modelled injury. To functionally evaluate the role of Vangl2 in bile duct fibrosis we used Vangl2 mouse mutants, which contain either a C-terminus point mutation in Vangl2 or conditional loss of the transmembrane domain of Vangl2 to knockout Vangl2 function.

Here we show that loss of Vangl2 results in a significant reduction of fibrosis following bile duct injury when compared to mice with intact Vangl2. The loss of Vangl2 demonstrates that it has a central and hitherto unidentified role in liver fibrosis. In mice where Vangl2 is abrogated we have defined that Vangl2 regulates a number of gene families associated with inflammation and have, furthermore, identified candidate pathways through which Vangl2 can potentially act. These data together highlight the role of the non-canonical Wnt signaling pathway in the maintenance of the fibrotic niche.

Moreover, with the use of therapeutic Wnt inhibitors we are able to modulate bile duct fibrogenesis and, for the first time, identify a targetable pathway for the treatment of PSC.

Lay Summary

The Liver is an essential organ, it plays a key role in metabolism but also fulfils other roles such as removal of red blood cells, detoxification, hormone production and the production of biochemicals used for digestion. The Liver is comprised of hepatocytes, which make up 70-85% of the liver's mass, and other cells such as stellate cells, portal fibroblasts, inflammatory cells and cholangiocytes. Cholangiocytes line the vessel walls of the bile ducts, these ducts carry bile from the liver to the duodenum to help with the digestion of fats. As with most cells or structures, cholangiocytes are susceptible to disease; these diseases are known as cholangiopathies. Primary Sclerosing Cholangitis (PSC) is a disease of the bile ducts that involves inflammation and damaging fibrosis. The cause of PSC is, as yet unclear, but is thought to be autoimmune related, where the body's own immune system attacks healthy cells. Inflammation of tissue surrounding the ducts leads to thickening of the vessel walls and narrowing of the duct itself and results in scar formation, thereby, leading to obstruction of bile flow. Over time, impairment of the duct accompanied by poor bile transport results in biliary fibrosis, progressive biliary cirrhosis and liver failure. PSC is increasing in prevalence, untreatable and, ultimately, requires transplantation. Given donor liver numbers have remained static over the last 30 years, investigating the causes of fibrosis, and targeting these therapeutically, is an attractive alternative to transplantation.

Signaling pathways throughout the cells of the body dictate their response to a multitude of stimuli. One of these pathways is the Wnt pathway. The signaling protein, Wnt, binds to a receptor and in some cases co-receptor. Wnt doesn't always bind to the same receptor nor does it always activate the same downstream signaling cascade within the cell when it binds to a receptor. Wnt signaling pathways can be grouped together based on some common features. One of these groups is the non-canonical Wnt signaling

pathway. The non-canonical Wnt signaling pathway has been shown to determine what defines the top and bottom of a cell as well as determining the direction of how cells move, giving cells direction and orientation. However, its role in adult tissue regeneration is poorly understood.

Here we use a mouse which has PSC to show an activation of the non-canonical Wnt pathway and downstream activation of this pathway. Particularly, we have found that non-canonical Wnt ligands and receptors are increased specifically in the regenerating ducts. We have then removed this pathway genetically in mice by deleting a protein known as Van Gogh-like-2 (Vangl2) and can show that fibrosis is reduced. Showing for the first time that the role of the non-canonical Wnt pathway in liver is to activate the formation of fibrosis. We are able to use very specific drugs that target the Wnt pathway and can show that treating with these drugs can modulate bile duct fibrogenesis and, for the first time, we have identified a targetable pathway for the treatment of PSC.

Table of Contents

Chapter 1: Introduction

1.1 The Liver

The liver acts as a vast chemical factory, synthesizing large complex molecules from low molecular weight substances brought to it in the blood particularly substances recently absorbed by the intestine and transported by a portal blood system. The liver also breaks down toxic substances brought to it by the hepatic artery, and synthesizes bile, which is transferred by a system of ducts (the biliary system) to the duodenum (Stanfield, 2012).

All of the biochemical functions of the liver are carried out by the epithelial parenchymal cell of the liver, the hepatocyte, and are dependent on complex inter-relationships between:

- The vasculature (hepatic artery and portal vein branches, sinusoids and central veins)
- The hepatocytes
- The bile drainage systems (the canaliculi and intrahepatic bile duct)

1.2 Vasculature

The liver receives blood from two vessels, the hepatic artery and the hepatic portal vein (Stevens & Lowe, 1996). The hepatic artery perfuses the liver with oxygenated blood from the celiac axis branches of the aorta. On entering the liver, it divides into increasingly smaller branches. The hepatic portal vein carries blood from the digestive tract that is rich in amino acids, lipids, and carbohydrates absorbed from the bowel, and also blood from the spleen, which is rich in haemoglobin breakdown products. After entering the liver at the

porta hepatis, the portal vein divides into smaller distributing veins, which then branch further, eventually forming terminal portal venules. In the liver, the two input circulations (hepatic artery and hepatic portal vein) discharge their blood into a common system of small vascular channels, the sinusoids, which are in intimate contact with the hepatocytes. The hepatic artery branches supply oxygenated blood containing metabolites for reprocessing and toxins for detoxification by hepatocytes (Stanfield, 2012; Stevens & Lowe, 1996).

Recently it has come to light that the hepatobiliary vasculature plays a key role in liver regeneration, with the hepatic vascular niche, predominantly represented by liver sinusoidal endothelial cells, initiating regeneration and determining the correct spatial and metabolic zonation of regenerating hepatocytes. Initially, this was highlighted by the discovery that upon ablation of VEGF-A receptor-2 in the liver sinusoidal endothelial cells inhibited the initial regenerative burst of proliferation within the hepatocytic population and subsequently limited the regeneration of the hepatocellular mass. It was found that the endothelial cell transcription factor *Id1* was key to the regenerative process driven by the liver sinusoidal endothelial cells. Knockout of *Id1* in mice showed the same phenotype due to reduced expression of liver sinusoidal endothelial cells angiocrine factors, one of which is Wnt2 and the other HGF, indicating for the first time that the hepatic microvasculature has an instructive role in ensuring the liver is able to regenerate appropriately (Ding et al., 2010).

1.3 Hepatocytes

The main functional cell of the liver is the hepatocyte; they are the parenchymal tissue of the liver making up 70-85% of the liver's mass. These cells are involved in protein

synthesis and storage, transformation of carbohydrates, synthesis of cholesterol, bile salts and phospholipids, detoxification, modification, and excretion of exogenous and endogenous substances and the initiation of formation and secretion of bile (Stanfield, 2012; Stevens & Lowe, 1996).

Hepatocytes (liver cells), which are intimately associated with the network of blood vessels (sinusoids), are polarized polyhedral cells with three identifiable types of surface (Eroschenko, 2012; Stevens & Lowe, 1996). The hepatocyte surfaces are important because they are involved in the transfer of substances between the hepatocyte, blood vessels and bile canaliculi. The three types of surface are sinusoidal, canalicular, and intercellular. Sinusoidal surfaces are separated from the sinusoidal vessel by the space of Dissé. They account for approximately 70% of the total hepatocyte surface. They are covered by short microvilli, which protrude into the space of Dissé. Between the bases of the microvilli are coated pits which are involved in endocytosis (Eroschenko, 2012; Stevens & Lowe, 1996). The sinusoidal surface is the site where material is transferred between the sinusoids and hepatocytes and diffusion across this boundary is highly efficient. Canalicular surfaces are the surfaces across which bile drains from the hepatocytes into the canaliculi. They account for approximately 15% of the hepatocyte surface and are closely opposed except at the site of a canaliculus, which is a tube formed by the exact opposition of two shallow gutters on the surface of adjacent hepatocytes (Eroschenko, 2012; Stevens & Lowe, 1996). The intercellular surfaces are the surfaces between adjacent hepatocytes that are not in contact with sinusoids or canaliculi. They account for about 15% of the hepatocyte surface. These intercellular surfaces are comparatively simple, but specialized for cell attachment and cell-to-cell communication via communicating junctions (Stevens & Lowe, 1996).

1.4 Intrahepatic Biliary Tree

Bile produced by hepatocytes passes into bile canaliculi. The bile canaliculi carry the bile back to the portal tracts, away from the parenchyma. As the canaliculi approach the bile ductules in the portal tracts, they open into short passages, the canals of Hering, lined by small cuboidal epithelial cells, cholangiocytes (Eroschenko, 2012; Stevens & Lowe, 1996). Cholangiocytes are the epithelial cells of the bile duct. They are cuboidal epithelium in the small interlobular bile ducts, but become columnar and mucus secreting in larger bile ducts approaching the porta hepatis and the extrahepatic ducts (Eroschenko, 2012).

In the healthy liver, cholangiocytes contribute to bile secretion via net release of bicarbonate and water. Several hormones and locally acting mediators are known to contribute to cholangiocyte fluid/electrolyte secretion. Examples would be secretin, acetylcholine and ATP (Stanfield, 2012). Maintenance of bile flow from the liver into the bowel is necessary for both hepatic health, but also is required for digestion of lipid.

1.5 Liver Fibrosis

Fibrosis in the liver is caused by the excessive deposition of extracellular matrix (ECM). It is based on the interactions of hepatic stellate cells, which generate matrix, and are the resident livers cell and conditional infiltrating cells, such as macrophages and neutrophils.

The ECM is comprised of secreted molecules that forms a structural and biochemical support niche to surrounding cells. Localized cells, which aggregate within the matrix secrete ECM components. Components can be classified into proteoglycans and non-proteoglycan polysaccharides, proteins and others components such as fibronectin and

laminin. Glycosaminoglycans are carbohydrate polymers that bind to proteins to form the proteoglycans. Common forms are heparin sulfate, chondroitin sulfate and keratin sulfate. Hyaluronic acid is an example of a non-proteoglycan. Proteins within the ECM are of particular interest as they are the most abundant component of the ECM and consititue what we commonly see as the fibrotic response. Two principle fibrotic proteins are collagen and elastin. Collagen is the most prolific of these scar-forming proteins and gives structural support., There are fourteen types of collagen (Type I-XIV) which can be sub-divided into 5 groups; fibrillar (Type I-III, V, XI), facit (Type IX, XII, XIV), short chain (Type VIII and X), basement membrane (Type IV) and other (Type VI, VII, XIII). These different collagens contribute to disease processes in diverse ways. Elastins provide elasticity, giving the tissue the ability to move in response to force and return to its original form and is another major component of scar formation, however has been shown to be highly resolvable. Although there are many cell types that generate ECM specific to their localization, fibroblasts are the most common cell type involved and arise from the differentiation of non-fibrogenic pre-cursor cells.

In terms of tissue regeneration, the extracellular matrix prevents the immune system reacting to the injury and responding with inflammation and scar tissue. The ECM also facilitates the surrounding epithelial cells to repair the tissue and has an instructive role in regeneration, providing many of the necessary signals for regeneration, thereby preventing the deposition of scar tissue. Fibrosis is a homeostatic occurrence that can exist between normal expression of ECM and extreme examples that can end in cirrhosis. This homeostatic process is an essential part of tissue maintenance and regeneration but excessive formation of scarring will lead the inefficient recovery of the tissue architecture or the generation of non-functional tissue. The homeostatic nature of fibrosis (i.e. its ability to form and then regress) during injury, maintains the liver's integrity and function. This

combined with the remarkable regenerative capacity of the liver epithelium enables the organ to recover to a healthy functional state from chronic damage. Of course, protracted, iterative injury results in irreversible damage with cirrhosis and is largely irreversible due to collagen cross-linking within the ECM. This is mediated by the oxidation of lysine residues in collagen and elastin that promotes their polymerization and achieving a form that the body cannot remove.

Following injury and disease hepatic stellate cells (HSCs) become activated by signals that promote transdifferentiation of the quiescent HSCs to a myofibroblastic phenotype (TGFβ, IL6). This activation is characterized by the expression of α-smooth muscle actin by fibroblasts and a parallel loss of retinoids and lipid droplets, a reduction in the expression of adipogenic/lipogenic factors, and de novo expression of receptors for pro-fibrogenic, pro-chemotactic, and mitogenic factors. These cells differentiate into a myofibroblast (MFB) phenotype and begin to express ECM components within the liver tissue. Since fibrosis is a homeostatic state, if the insult is temporary and the injury quickly resolved, then these changes are transient. However, a sustained insult with chronic inflammation would lead to persistent and long-term activity of HSCs and MFBs and would result in the chronic accumulation of ECM. This accumulation inhibits liver function by the disruption of normal liver architecture and the substation of liver parenchyma with scar tissue, resulting in reduced function in the tissue.

ECM homeostasis can be further perturbed in chronic liver disease by the disruption in activity of matrix metalloproteinases (MMPs) and their corresponding inhibitors (TIMPs). MMPs encompass a family of zinc- and calcium-dependent enzymes whose role is to degrade ECM proteins and thus maintain homeostasis. Activated HSCs and MFBs have been identified as sources of MMPs and TIMPs (Ramachandran & Iredale, 2012).

1.6 Cholangiopathies

Cholangiopathies, account for 18% of all adult liver transplants and the vast majority of paediatric cases. Cholangiopathies are a group of chronic liver diseases in which the biliary epithelium becomes occluded or damaged leading to the formation of scar tissue surrounding the bile duct (Nakanuma, 2012) .

Cholangiocytes are able to proliferate in response to endogenous or exogenous signals/stimuli and play a key role in inflammatory and reparative processes within the liver (Glaser & Gaudio, 2009; Greenbaum & Wells, 2011). Furthermore, cholangiocytes interact with the immune system and microorganisms and are involved in drug metabolism. To accomplish these multifaceted functions, cholangiocytes display morphologic and functional heterogeneity along the biliary tree. Cholangiocytes lining large bile ducts (300 – 800μm) participate in hormone-regulated bile secretion, whereas cholangiocytes lining small bile ducts (15–300μm) possess proliferative capabilities and display considerable plasticity, being able to assume a "reactive phenotype" in disease conditions and potentially house the liver progenitor cell, the oval cell. Cholangiocytes represent the primary cell target of a diverse group of genetic and acquired biliary disorders collectively referred to as cholangiopathies. Many of the cholangiopathies are, at their early stages, site restricted along the biliary tree. For instance, primary biliary cholangitis (PBC), drug-induced cholangiopathies, and graft vs. host disease (GVHD) involving the liver affect primarily the small bile ducts. In contrast, primary sclerosing cholangitis (PSC) mainly involves the large intra- and extrahepatic bile ducts (Fava, 2010; Nakanuma, 2012). Thus, recognition of cholangiocyte heterogeneity along the biliary tree is necessary to understand better the cholangiopathies and, potentially, to devise novel, effective therapies. Because of their morbidity, mortality, need for liver transplantation, and overall cost to society, cholangiopathies are now recognized as an important group of liver diseases. Most

cholangiopathies display a progressive course leading to cirrhosis and liver failure. To date, the cause of most cholangiopathies remains obscure, although current thought seems to be settling on them being triggered by autoimmunity, thus treatment for these diseases remains under developed, with liver transplant offering the only curative option to treat these diseases.

1.7 3,5-diethoxycarbonyl-1,4-dihydrocollidine (DDC), a xenobiotic model of bile duct injury

3,5-diethoxycarbonyl-1,4-dihydrocollidine (DDC) acts by inducing increased porphyrin secretion and its deposition in the form of occluding plaques in bile ducts. This leads to inflammation surrounding the ducts and subsequently fibrosis. DDC is widely used to investigate Mallory body formation, as seen in alcoholic liver disease, as well as oval cell activation and proliferation. Oval cells are bipotential stem cells that reside within the canals of Hering. They can differentiate into either hepatocytes or cholangiocytes. A murine model of bile duct disease requires the supplementation of standard diet with DDC and shows a strong ductular reaction, which increases over time. In biliary cells the expression of vascular cell adhesion molecule (VCAM), osteopontin, TNF-α, Notch and Hedgehog are upregulated following the administration of DDC. Histopathologically, dietary administration of DDC leads to small duct sclerosis with infiltration of inflammatory mononuclear cells and activation of portal fibroblasts, causing biliary liver fibrosis. Murine liver challenge with DDC is a suitable model of primary sclerosing cholangitis in humans as the biliary inflammation, ductular and cellular response around the bile ducts seen in DDC mirrors that found in PSC (Fickert et al., 2007, 2014; Stöger et al., 2006).

1.8 Wnt Signaling Pathways

Wnt signaling was first identified in 1982 under the name Int1 (R Nusse, van Ooyen, Cox, Fung, & Varmus). It was subsequently shown to be evolutionarily highly conserved across species and had was characterised as Wingless (Wg) in *Drosophila* (R. van Amerongen & Nusse, 2009). Since it was understood that Wg functioned as a segment polarity gene involved in body axis formation, it was thought that Int1 (Wnt) would also be involved in embryonic development. Wnt signaling is a classic evolutionarily conserved pathway, it is consistently demonstrated to play an influential role in organisms particularly in embryonic development, tissue homeostasis and disease, where cellular proliferation and differentiation is required.

Wnt signaling pathways fall into three categories, the canonical Wnt/β-catenin dependent, the non-canonical pathway, this pathway is β-catenin independent and the Wnt/Ca^{2+}pathway, which is also independent of β-catenin (Niehrs, 2012). The β-catenin dependent pathway has been thoroughly characterised in key model species. Activation of the canonical pathway results in inhibition of β-catenin's destruction complex and thus an accumulation of β-catenin in the cytoplasm and its translocation to the nucleus, where it acts as a coactivator of transcription factors belonging to the TCF/LEF family. The Wnt/ β-catenin pathway regulates stem cell pluripotency and cell fate decisions during development. However, the same thoroughness and level of description cannot yet be said for the non-canonical pathways that remains grossly under-described and characterised especially in adult tissue homeostasis and disease.

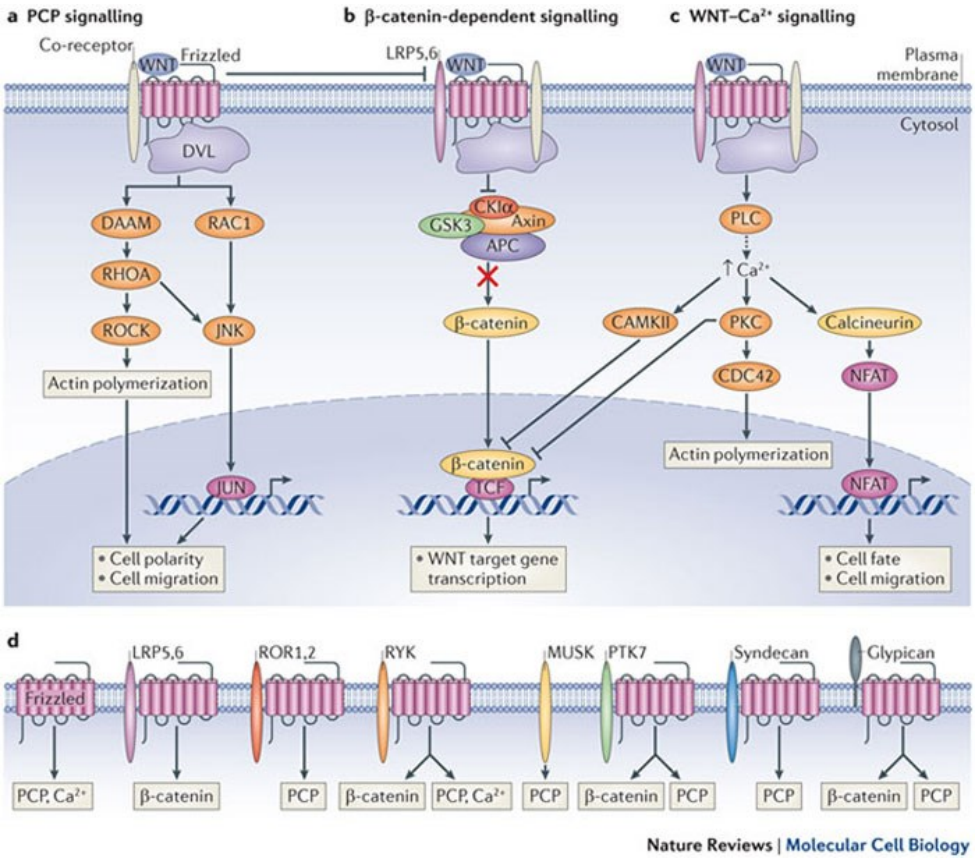

Figure 1 A simple diagrammatic representation by Niehrs *et al* (2012) outlining the three commonly referred to forms of Wnt signaling pathways. The Canonical, or β-Catenin dependent, pathway (B), the Calcium dependent Wnt-Ca^{2+} pathway (C) and the Non-Canonical, or what is often referred to as the PCP (Planar Cell Polarity) pathway (A). It also highlights the breadth of receptors and co-receptors that have been described as responding to Wnt ligands. These are but a small number of the more well described.

1.9 The Non-Canonical Wnt Mediated Pathways

The non-canonical Wnt-mediated pathways are identified as operating independently from β-catenin. Historically, this has always been considered to be the Wnt-Ca pathway and the Planar Cell Polarity Pathway (PCP). Fittingly, for a poorly described sibling of the canonical pathway there are, it seems multiple Wnt mediated, yet β-catenin-independent pathway descriptions: Wnt-RAP1 signaling pathway, Wnt-Ror2 signaling pathway, Wnt-PKA pathway, Wnt-GSK3MT pathway, Wnt-aPKC pathway, Wnt-RYK pathway, Wnt-mTOR pathway, and Wnt/calcium signaling pathway. However, the task of deciphering their presence and roles is increasingly challenging as they can all show a degree of overlap between pathways and utilize common receptors and activate similar downstream pathways by activating transcription factors and antagonizing other signaling pathways.

Frizzled (Fzd) is a G-protein coupled receptor best known as a receptor for the Wnt family of secreted proteins (Takeuchi et al., 2003). Activation of the Fzd receptor can be achieved by Wnt alone however this is a rare occurrence and more commonly a co-receptor is employed to achieve activation. In the canonical signaling pathway, the receptor LRP functions as a co-receptor. In the non-canonical Wnt signaling pathway the possible combination of co-receptors is much more extensive and include receptor and receptor-like tyrosine kinase (Ryk), ROR1/2, NRH1 or PTK7 (Zallen, 2007). Wnt protein binds to the N-terminal extra-cellular cysteine-rich domain of Fzd (Takeuchi et al., 2003) (McNeill & Woodgett, 2010). The activated receptor complex then recruits Disheveled (DVL) from the cytoplasm, which uses its PDZ and DEP domains to form a complex with Disheveled-associated activator of morphogenesis 1 (DAAM1) (McNeill & Woodgett, 2010). This triggers the activation of the small GTPases RHOA and RAC1, which in turn activates RHO-

associated kinase (ROCK) and JUN-N-terminal kinase (JNK) (McNeill & Woodgett, 2010; Zallen, 2007). This leads to actin polymerisation, microtubule stabilisation as well as JNK-c JUN/cFOS dependent transcription (Cui, Capecci, & Matthews, 2011a; Takeuchi et al., 2003).

Recently, the distinction of the Wnt signaling pathways as separate and independent has come under debate with some evidence being published proposing interaction across pathways. This was highlighted with Wnt5a being shown to both activate Wnt/β-catenin via the canonical pathway but also that it's activation of the non-canonical PCP pathway represses the canonical signalling pathway (Kawano & Kypta, 2003; V. Amerongen, Fuerer, Mizutani, & Nusse, 2012).

1.10 Vangl2

Mammalian Vangl2 is a highly conserved transmembrane protein commonly associated with the Planar Cell Polarity Pathway, a non-Canonical Wnt mediated pathway (Niehrs, 2012). It evolved from a single ancestral protein identified in Drosophila as Strabismus (Katoh, 2002). Vangl2 is involved in early morphogenesis, patterning of both axial midline structures and the development of the neural plate. Vangl2's involvement in the PCP pathway was observed in the orientation of stereociliary bundles in the cochlea (Mlodzik, 2010), where loss of Vangl2 results in disorientation of stereocillia hairs. Vangls are known to act as a co-receptors with Fzd to receive Wnt ligand (Gray, Roszko, & Solnica-Krezel, 2011; Hatakeyama, Wald, Printsev, Ho, & Carraway, 2014). Of particular interest to the field at the moment, and the focus of current research in a number of groups, is the evidence supporting the role of ROR2 and/or PTK7 in forming a Wnt-induced non-canonical signaling complex with Vangl2 which results in the phosphorylation of Vangl2 (Gao et al.,

2011; Martinez et al., 2015; Mouri et al., 2014). This interaction has been found to be Wnt dose-dependent. Furthermore, a similar relationship has been found to exist between Ryk and Vangl2 (Macheda et al., 2012). These interactions demonstrate a pathway whose description is still in its infancy and yet points to a series of complex interactions underpinning a variety of developmental, regenerative and physiological processes.

There are two mouse homologs of Drosophila Stbm/Vang gene, Vang-like 1 (Vangl1) and Vang-like 2 (Vangl2)(Katoh, 2002). The Vangl genes encode a four-transmembrane domain protein with a C-terminal PDZ domain. Vangl2 is mutated in the Looptail (Lpt) mouse, a missense mutation on Chromosome 1 confers a point mutation and a non-synonymous amino acid change at the C-terminal cytoplasmic domain of Vangl2 that originated spontaneously and leads to destabilisation of the resulting protein (Yin, Copley, Goodrich, & Deans, 2012). Mice exhibiting heterozygosity for Vangl2 demonstrate a number of non-lethal phenotypes the most striking of which is a looped or kinked tail hence the commonly used term to describe them, Looptail. The Lpt mutation causes a failure in neural tube closure (craniorachischisis) in homozygous mutant animals, implicating a defect in the developmental role of the PCP pathway (Doudney & Stanier, 2005; Torban, Wang, Groulx, & Gros, 2004). Extensive work has been done on the role of the PCP pathway and in particular Vangl2 during cochlear development using the Lpt mouse model. The Lpt mice display pronounced polarization defects in the orientation of stereociliary bundles in the inner and outer hair cells of the mouse cochlea; this provided one of the first pieces of evidence supporting the existence of a conserved PCP pathway in the mammals (Montcouquiol et al., 2006; Zallen, 2007). The characterization of Lpt mice in the PCP regulation of the cochlea is highly significant and establishes the Lpt mice as a classic mouse model for PCP study. The Lpt mice have been used extensively for subsequent PCP studies to test genetic interactions in PCP signaling and to validate novel PCP genes.

Chapter 2: Aims, Hypothesis and Rationale

Aim 1: Isolate and enrich for bile ducts from whole liver tissue.

I predict that isolating bile ducts form whole liver will improve analysis of a relatively small population of cells.

Bile ducts comprise a relatively small population of the whole liver. To ensure accurate analysis of the cells that comprise this structure it would be important to attempt to isolate or enrich for them to avoid the parenchymal cells masking or contaminating the output data. This holds particularly true if the marker or signal of interest is lowly expressed or if any hypothetical change occurring is small in the context of the whole organ but significant in the bounds of the ductual structure.

Characterise Vangl2 and components of the non-canonical Wnt pathway in the liver during injury.

I predict that the non-canonical Wnt pathway is activated during bile duct injury.

The non-canonical Wnt mediated pathway and Vangl2 are, relatively, poorly described in the literature. There is some sparse evidence that it may play a role in the liver during injury. To investigate it is important to analyze the tissue under normal conditions and using an induced injury model to attempt to identify any changes that occur.

Aim 3: Investigate the response to modulation of Vangl2 in the liver during injury with the Looptail mouse.

I predict that by using the Looptail mouse to modulate Vangl2's activity we will gain insight into the role the non-canonical Wnt pathway plays during injury.

By modulating Vangl2 we can observe the influence it has during injury on the downstream activity its activation induces.

Chapter 3 – Materials and Methods

3.1 Animal lines used in this study.

All animals used in this study were housed in 12h light/dark cycles. When mice were not on an injury protocol they were maintained on RM1 animal food and normal drinking water. Male mice, aged 8 weeks, were used to model bile duct injury and regeneration. CD1 mice were used for all studies involved in defining changes during the experimental time-course and were bred in-house. Looptail (Lpt) mice, which contain a Vangl2 S464N mutation were imported from MRC Harwell, Oxford. These mice were supplied on a C3H background and were maintained at heterozygous crosses with C3H companion mice. All mice were fed 0.1% 3,5-diethoxycarbonyl-1,4-dihydrocollidine (DDC) food, made up in RM1 base feed for up to 14 days. Animals were maintained in accordance to UK Home Office regulations.

3.2 Dissection and Fixation of Tissue.

Adult mice were sacrificed by CO_2 and cervical dislocation or exsanguination at the defined experimental endpoint. The liver was flushed through with PBS by rapid infusion through the inferior vena cava and out through the portal vein before tissues are dissected out from the animal. Tissue was fixed in 4% PFA for 24 hours then transferred to 75% Ethanol for 24 hours. Tissue was then processed for paraffin wax embedding using a Tissue-Tek VIP unit.

Tissue sections were cut on a Leica RM2235 Manual Microtome at 3µm thickness, floated in a water bath and mounted on ThermoFisher Superfrost slides before being heated at 65°C for at least 20mins.

For tissues which are to be used for RNA extraction, tissue was snap frozen using 2-methylbutane super-chilled with dry ice. This tissue was stored at -80°C for future use.

3.3 Picro-Sirius Red staining of total fibrillar collagen.

3µm sections on glass slides were dewaxed through 3 consecutive washes of Xylene for 5minutes each. Following this the sections were rehydrated through decreasing concentrations of alcohol (100%, 90%, 75%, 50%) for 5 minutes each before finally being washed in water. The nuclei were staining using Mayer's Haematoxylin for 10 minutes then washed in warm running water for 5 minutes. The sections were placed in picro-sirius red solution for 6 minutes. Upon reaching equilibrium staining the sections were rinsed in two changes of acidified water. The sections were dehydrated in three changes of 100% alcohol and cleared in 3 changes of Xylene for 5 minutes each. The sections were mounted with glass cover slips using DPX.

Picro-Sirius Red Solution

Sirius Red F3B	0.5g
Saturated aqueous picric acid	500ml

Acidified Water

5ml Glacial acetic acid in 1 litre water

3.4 Immunohistochemistry Protocol

3µm sections from mouse liver fixed in 4% PFA. Sections were dewaxed in Xylene for 3 x 5 minutes before being rehydrated through alcohol (100%, 90%, 75%, 50%) for 5 minutes each before finally being washed in water. If necessary antigen retrieval and proteinase K digestion was carried out. Sections were washed in PBS for 5 minutes. Before being incubated in 3% hydrogen peroxide for 20 minutes at room temperature. The sections were mounted in a Sequenza staining rack. Sections were incubated with 120µl avidin blocker for 15 minutes at room temperature and then washed with 3 rinses of PBS for 5 minutes each. The sections were then incubated with 120µl biotin blocker for 15 minutes at room temperature. The sections were then blocked for non-specific protein with a protein blocker for at least 30 minutes. 120µl of diluted primary antibody in antibody diluent was added to each slide and incubated at 4 ºC overnight. The sections were then rinsed in 3 changes of PBS for 5 minutes each. 120µl of diluted secondary antibody in antibody diluent was added to each slide and incubated for 1 hour at room temperature. The sections were, once again, rinsed in 3 changes of PBS for 5 minutes each. 3 drops of Vector RTU ABC reagent were added to each slide and incubated for 30 minutes att room temperature. Sections were rinsed 3 times in PBS for 5 minutes. 200µl of DAB reagent was added to each slide and incubated for up to 10 minutes depending on the intensity of staining required. The slides were rinsed with water and transferred to a rack and were counter-stained with Harris's Haematoxylin for up to 30 seconds before being rinsed with running water and "blued" in Scott's Tap Water. Finally, the sections were dehydrated through Alcohol, cleared in Xylene and mounted with DPX.

3.4.1 Antigen Retrieval

0.01M Citrate Buffer pH 6.0. 5 mins in microwave on high

Tris-EDTA Buffer (10mM Tris Base, 1mM EDTA Solution, 0.05% Tween 20, pH 9.0) Pre-heated for 5 mins in microwave then 2x5mins on high

3.4.2 Proteinase K digestion

6.25mg in 50 ml PBS @ 37ºC for 5 mins. Stock proteinase K = 25mg/ml

3.4.3 Primary Antibodies

Antigen	Species	Clone	Catalogue #	Company	Dilutions	Ag Retrieval
aSMA	Mouse	1A4	A2547	Sigma	1/2000	15m NaCt
Collagen-1	Goat		1310-01	SouthernBiotech	1/200	15m NaCt
Desmin	Rabbit		ab8592	Abcam	1/100	15m NaCt
PTK7	Rabbit		17799-1-AP	Proteintech	1/100	15m TE
Vangl2	Rabbit		HPA027043	Sigma	1/100	10m TE
Wnt5a	Rabbit		LS-B4565	LS Bio	1/100	20m NaCt

3.4.4 Secondary Antibodies

Rabbit anti-Goat IgG (H+L) Secondary Antibody, Biotinylated Vector, 1/500

Goat anti-Rabbit IgG (H+L) Secondary Antibody, Biotinylated Vector, 1/500

Rabbit anti-Mouse IgG(H+L) Secondary Antibody, Life Technologies, 1/200

Goat anti-Rabbit IgG (H+L) Secondary Antibody, HRP conjugate, Vector 1/500.

For fluorescence, following secondary incubation sections were incubated with tyramide-555 as per the manufacturer's instructions. They were then heat treated with TE for 10m

and second primary antibodies were incubated with tissue followed by a second round of HRP secondary. This was then incubated with tyramide-488.

3.5 mRNA isolation

Snap frozen tissue was cut from the main block with a scalpel on dry ice. Tissue was homogenised using a Qiagen TissueRupter in 0.5ml Trizol LS (Amersham) for 5 minutes. The homogenate was briefly spun and mixed with one-fifth the volume of chloroform and vortexted for 30s. Chloroform and Trizol LS separate, and RNA is isolated from the aqueous phase. Trizol/Chloroform mixtures were spin at 12,000G for 15m at 4^{o}C following which the aqueous phase is collected to a separate tube. The aqueous phase is mixed, 1:1 with isopropanol (Propan-2-ol) to precipitate RNA. This precipitated RNA is then applied to a Qiagen Micro kit tube and the protocol followed. Briefly, we washed the membrane with a wash of RW1 buffer followed by two washes of RPE. Membranes were spun to dry and then rehydrated with between 30 and 50µl RNAse/DNAse free dH2O.

3.6 Reverse Transcription

A Nanodrop was used to quantify the concentration of RNA in the sample. 1µg of RNA was made up to 12µl using dH_2O. 2µl of Qiagen gDNAse is added and the solution vortexed to mix. The resulting mixture is incubated at 42^{o}C for 5 minutes and then placed on ice for 2 minutes. 5µl of premixed random primers and mastermix was added. 1µl of reverse transcriptase was also added. Using a thermocycler the reaction was incubated at 42^{o}C for 30 minutes followed by 95^{o}C for 3 minutes, to inactivate any remaining enzyme.

The cDNA samples can then be stored on ice for immediate use or frozen at -20^{o}C for use at a later date.

3.7 Quantitative PCR

All Primer sets were provided by Qiagen and detailed in the table below:

Gene	Species	Company	Product	Cat. #
ABCB1	Mouse	Qiagen QuantiTect	Mm_Abcb1b_1_SG QuantiTect Primer Assay	QT00140945
Albumin	Mouse	Qiagen QuantiTect	Mm_Alb_1_SG QuantiTect Primer Assay	QT00115570
Dvl1	Mouse	Qiagen QuantiTect	Mm_Dvl1_1_SG QuantiTect Primer Assay	QT00106393
Dvl2	Mouse	Qiagen QuantiTect	Mm_Dvl2_1_SG QuantiTect Primer Assay	QT00112154
Dvl3	Mouse	Qiagen QuantiTect	Mm_Dvl3_1_SG QuantiTect Primer Assay	QT01079092
Fzd1	Mouse	Qiagen QuantiTect	Mm_Fzd1_1_SG QuantiTect Primer Assay	QT00290542
Fzd2	Mouse	Qiagen QuantiTect	Mm_Fzd2_1_SG QuantiTect Primer Assay	QT00261485
Fzd3	Mouse	Qiagen QuantiTect	Mm_Fzd3_1_SG QuantiTect Primer Assay	QT00147917
Fzd4	Mouse	Qiagen QuantiTect	Mm_Fzd4_1_SG QuantiTect Primer Assay	QT00260526
Fzd6	Mouse	Qiagen QuantiTect	Mm_Fzd6_1_SG QuantiTect Primer Assay	QT00109998
Fzd7	Mouse	Qiagen QuantiTect	Mm_Fzd7_1_SG QuantiTect Primer Assay	QT00307797
Fzd8	Mouse	Qiagen QuantiTect	Mm_Fzd8_2_SG QuantiTect Primer Assay	QT02328151
Hnf1b	Mouse	Qiagen QuantiTect	Mm_Hnf1b_1_SG QuantiTect Primer Assay	QT00103320
Hnf4a	Mouse	Qiagen QuantiTect	Mm_Hnf4a_1_SG QuantiTect Primer Assay	QT00144739
Krt19	Mouse	Qiagen QuantiTect	Mm_Krt19_1_SG QuantiTect Primer Assay	QT00156667
Ptk7	Mouse	Qiagen QuantiTect	Mm_Ptk7_1_SG QuantiTect Primer Assay	QT00144032
Ror2	Mouse	Qiagen QuantiTect	Mm_Ror2_1_SG QuantiTect Primer Assay	QT00172872
Ryk	Mouse	Qiagen QuantiTect	Mm_Ryk_1_SG QuantiTect Primer Assay	QT00171724
Sox9	Mouse	Qiagen QuantiTect	Mm_Sox9_1_SG QuantiTect Primer Assay	QT00163765
Vangl1	Mouse	Qiagen QuantiTect	Mm_Vangl1_1_SG QuantiTect Primer Assay	QT00494235
Vangl1	Human	Qiagen QuantiTect	Hs_VANGL1_1_SG QuantiTect Primer Assay	QT00072548
Vangl2	Mouse	Qiagen QuantiTect	Mm_Vangl2_1_SG QuantiTect Primer Assay	QT00128422
Vangl2	human	Qiagen QuantiTect	Hs_Vangl2_1_SG QuantiTect Primer Assay	QT00512050
Wnt4	Mouse	Qiagen QuantiTect	Mm_Wnt4_1_SG QuantiTect Primer Assay	QT00104622
Wnt5a	Mouse	Qiagen QuantiTect	Mm_Wnt5a_1_SG QuantiTect Primer Assay	QT00164500
Wnt11	Mouse	Qiagen QuantiTect	Mm_Wnt11_1_SG QuantiTect Primer Assay	QT00103663

The reaction was made up as below (per reaction):

5ul (50ng) of cDNA

1.25ul Quantitect Primer Assay

6.25ul Roche SYBR mastermix.

qPCR was run in triplicate in a 384-well format using a Roche lightcycler 480-II, for 40 cycles. The cycling conditions were as follows:

	Cycles	Analysis	Target	Hold	Ramp
Pre-Incubation	1	None	95°C	5mins	4.8°C/s
Amplification	45	Quantification	95°C 60°C 72°C	10s 10s 15s	4.8°C/s 2.8°C/s 4.8°C/s
Melting Curve	1	Melting Curves	95°C 65°C 97°C	5s 5s 1min 1s	4.8°C/s 2.5°C/s
Cooling	1	None	40°C	5mins	

All data was analysed using the $2^{\Delta\Delta Ct}$ analysis method and normalised to uninjured controls or wild-type controls.

3.8 RNAScope In Situ Hybridisation:

RNAScope insitu hybridization was performed by Aquila Histoplex. The Boulter Lab provided blocks of tissue for processing and staining.

3.9 Bile Duct Isolation and Organoid Culture

Freshly flushed and dissected liver was cut into small pieces and immersed in dissociation media (12.5mg collagenase type XI (Sigma C9407), 12.5mg dispase (gibco 17105-041) in 100ml DMEM 1% FBS) and incubated at 37°C in a water bath. The tissue fragments were agitated every 30mins using a 10ml automated pipette. The dissociation media was refreshed every hour for the first 2hours. After this time the supernatant was checked for ducts being present. When no ducts are present the supernatant can be pipetted off and disposed. When the ductual structures start to appear transfer the tissue suspension through an inverted 70µm cell strainer, re-invert the strainer into a 50ml tube and flush with media. This sample is now enriched for ductal structures and can be snap frozen and stored or used immediately as required.

For organoid culture, transfer the supernatant to a 10cm dish and examine under a microscope at low magnification. Any ducts present can be transferred by hand using a pipette to a 15ml tube containing DMEM Glutamax with 5% FCS and 5% P/S. Centrifuge the collected ducts at 300g for 5mins and remove the supernatant. The pellet is then re-suspended in 10ml of media without growth factors (Advanced DMEM/F12 with Glutamax, Hepes, P/S). Centrifuge the washed ducts again at 300g 2-3mins and remove the supernatant and put the collected pellet on ice. Add 20µl/well of Matrigel to the pellet and pipette gently to disrupt the pellet and re-suspend in Matrigel. Pipette 20µl into each well of a pre-warmed plate, the tip should be held off the base of the well so as to form a dome of matrigel containing suspended ducts, and transfer to an incubator for 10mins. Once the matrigel has solidified add 300-500µl of growth factor expansion media (Advanced DMEM/F12 with Glutamax, Hepes, P/S, mEGF, R-Spondin, Gastrin, Wnt3a, FGF10, HGF, n-Actelycysteine, B27, A83-01 (TGFβ inhibitor), CHIR99021 (GSK Inihibitor), ROCK Inhibitor,

Forskolin) and return to the incubator. Organoids were fed every 2-3 days. The organoids were passaged using a mechanical dissociation method. The media was aspirated from each well and replaced with 300-500µl of chilled Versene. The Organoids were removed by pipette and agitated in the Versene. The re-suspended organoids were centrifuged at 300g for 5mins and the Versene removed. The pellet was re-suspended in chilled PBS and centrifuged at 300g for 5mins. Depending on the number of wells being passaged and volume of Matrigel removed it may be necessary to wash more than once to remove the Matrigel from the pellet. The Pellet can then be re-suspended as before in fresh Matrigel and the organoid fragments plated out as before in clean wells.

Chapter 4 – Isolation and culture of adult bile ducts to model the function of Vangl2

4.1 Overview of Enrichment and Isolation of Bile Ducts

The presence of Vangl2 and its signaling pathway members has not been examined in adult tissues before and there is little information Vangl2 expression in the liver. However, a single paper investigating the pathway in zebrafish indicated that Vangl2 and Vangl1 are important for duct generation. Therefore, to determine whether Vangl2 is expressed specifically in the bile ducts I sought to develop a method of enriching for bile ducts. Moreover, I wanted to be able to functionally use these ducts for over-expression and knockdown of Vangl2. To do this I needed to establish a bile duct organoid culture method in the lab, which had not been done before.

Up to 85% of the mass of the liver is comprised of hepatocytes and non-bile duct cell types, it was therefore key to be able to enrich our samples for cholangiocytes and bile ducts prior to trying to establish bile duct organoid lines. Previous studies have shown that enrichment for cholangiocytes using cell surface markers, such as EpCAM, CD133 and CD24 can isolate single cells and that these can form organoids in vitro. However, there are limitations to these methods; they are incredibly time-consuming, these markers do not necessarily represent the cellular diversity seen within the bile duct, and likely select for a primitive population of cells and the number of bile ducts organoids generated is relatively low.

To this end, I developed a bile duct extraction protocol based on the original methodology by Huch *et al*. Briefly, whole livers were flushed with PBS through the Inferior Vena Cava (IVC) and dissected into PBS. During the development of this protocol I found

that roughly slicing them into smaller pieces was more effective than finely slicing them as the fragments of bile ducts that were ultimately generated were more substantial, due to this the ducts could be identified and isolated more easily and therefore many more organoids could be generated per section of duct. To remove hepatocytes from these tissue fragments I incubated the tissue in DMEM/Hams-F12 with dispase and collagenase. By pipetting these tissue slices up and down could disaggregate the hepatocytes from the biliary tree, but largely maintain the structure and cellularity of the bile ducts. The hepatocytes were dissociated from the ducts over several hours and changes of media with repeat pipetting. By the end of this process, almost all of the hepatocytes have been lost to the media changes and what remains are bile ducts and single cells. To further enrich for the ductal population the digested livers were passed through a 70µm filter to remove single cells leaving only ducts. These ducts could then be used for further analysis and culture.

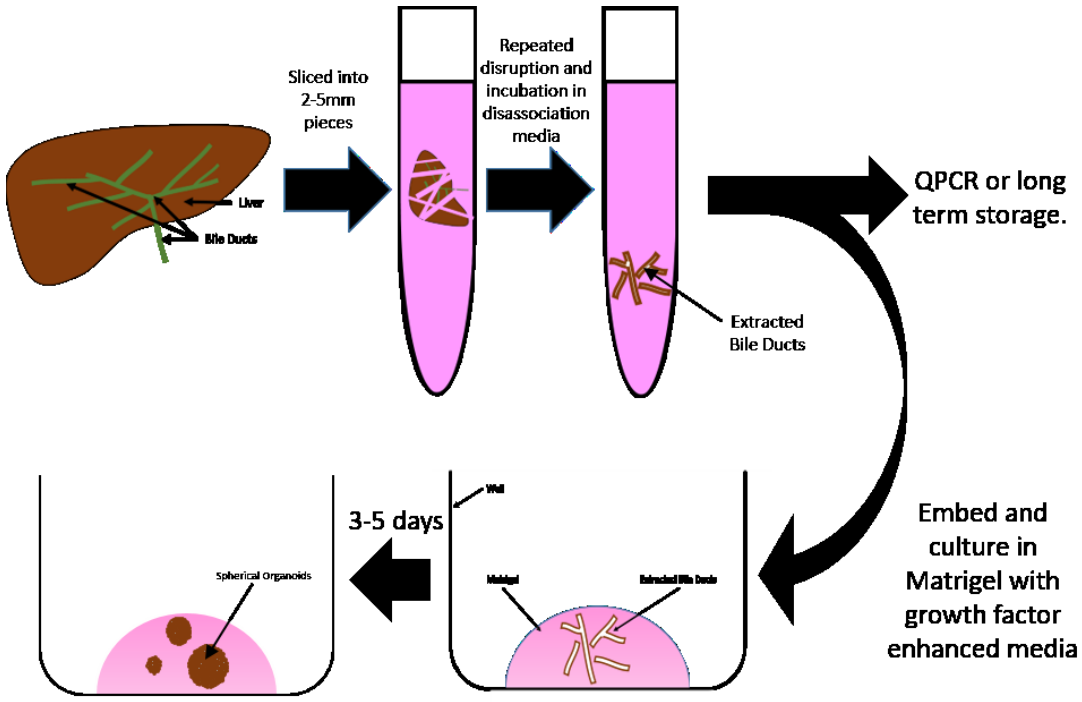

Figure 4.1 A diagrammatical representation of bile duct extraction. Whole liver is roughly sliced and through repeated incubations in disassociation media the parenchymal cells are removed to leave the bile ducts intact. The extracted ducts can be used immediately or stored for use at a later date. For organoid generation the ducts are embedded in Matrigel and supplied with a growth factor enhanced culture media. Within 24hours the extracted ducts "cap off" their open ends, by 48 hours small cystic-like buds can be seen on the ducts. After 3-5 days spherical organoids of a variety of sizes will be present while the original ductual structure will no longer be visible.

4.2 Validation of the Bile Duct Enrichment Protocol

My method of bile duct enrichment produces a visible population of ducts from whole liver by the sequential removal of parenchymal cells. I wanted to confirm this to determine that I have indeed enriched for bile ducts and also to try and determine what the level of contamination is, by hepatocytes, in the bile duct fraction following enrichment. To do this I took a portion of liver and isolated mRNA from this. The remaining liver was then subjected to my bile duct isolation protocol and bile ducts were enriched. These bile ducts were washed with PBS and then pelleted, lysed and mRNA was extracted. Using RT-qPCR I investigated a number of hepatocyte and bile duct markers to determine whether certain components of markers are enriched in particular fractions.

Cytokeratin 19 (KRT19) is a key marker of bile ducts. The Keratin gene family are important for intracellular stability in epithelial tissue with different members of the family displaying organ or tissue specific expression patterns. Keratin 19 (KRT19) is a Type-I keratin expressed in simple epithelia. Clinically, keratin 19 is used together with keratin 18 to distinguish between hepatocellular carcinoma and cholangiocellular carcinoma. Both keratins are expressed in bile ducts, but only keratin 18 is expressed in hepatocytes. This makes it an ideal marker for bile duct identification. Canalicular ATP-binding cassette (ABC) transporters are responsible for bile formation and secretion of bile acids, bilirubin and cholesterol. ABCB1 is responsible for the biliary excretion of xenobiotics across the canalicular membrane. There are some descriptions that indicate this is a hepatocyte expressed gene, however given the bile duct canaliculus represents the interface between the bile duct and the hepatocyte plate other studies have defined it as a biliary marker. I also selected Hnf1β as a candidate bile duct transcription factor since in development

Hnf1β knock-out mice fail to generate bile ducts and as such it, along with HNF6 are seen as archetypal biliary transcription factors.

To determine the levels of parenchymal contamination I chose albumin and HNF4α, both of which are known to be restricted to hepatocytes. Hepatocytes manufacture albumin to maintain the oncotic pressure of plasma. Hence, albumin represents a marker present in hepatocytes and highly expressed in whole liver but absent in bile ducts. Hepatocyte nuclear factor 4α (Hnf4α) is a transcription factor in hepatocytes that controls expression of liver secreted glycoproteins; it is not expressed in bile ducts. It is necessary for hepatocyte development and differentiation and is largely seen as the archetypal hepatocyte transcription factor.

Sox9 is also restricted to the adult biliary tree, so I chose to look at this following isolation. However, there are also reports that Sox9 is expressed in periportal hepatocytes.

By carrying out RT-qPCR, I found that the level of transcript for markers of the bile ducts, Krt19 ($p=<0.0001$) (Fig.4.2A) and ABCB1 ($p=0.0002$) (Fig.4.2B) are significantly higher in the bile duct enriched fraction compared to total liver. Interestingly, Sox9 ($p=0.0889$) (Fig.4.2F) is also enriched, but not significantly, and Hnf1β ($p=0.0068$) (Fig.4.2D) is expressed in whole liver and reduced, by comparison in the ductal sample. This is curious, however could represent for Sox9 at least that there is a sufficient level of Sox9 in the parenchymal cells in the liver, therefore total levels in both hepatocyte and cholangiocyte populations is high. Our data on Hnf1β is more surprising given its role in development, however given that these livers are homeostatic and the bile ducts are not turning over particularly, it could be that Hnf1β is not being actively transcribed and therefore its abundance in the bile ducts is relatively low.

We also found that the hepatocyte markers, albumin (p=<0.0001) (Fig.4.2C) and Hnf4α (p=<0.0001) (Fig.4.2E) are significantly over expressed in the whole liver samples compared to the bile duct samples, in which there was almost no detectable expression of either hepatocyte transcript.

From these data I can show that my duct enrichment protocol significantly improves the isolation of a population of ductal cells. It is clear microscopically that this protocol does not produce immaculately clean ducts and that there are likely some hepatocytes remaining in these preparations which have not been digested away, however it is a balance between maintaining the duct tissue and this contamination. However, based on this RT-qPCR data this is a not an issue for using this protocol in future experiments however data generated from tissue which has been enriched for ducts should also be validated with IHC or RNA in-situ in tissue to confirm that expression is not due to hepatocytes which remaining post dissociation.

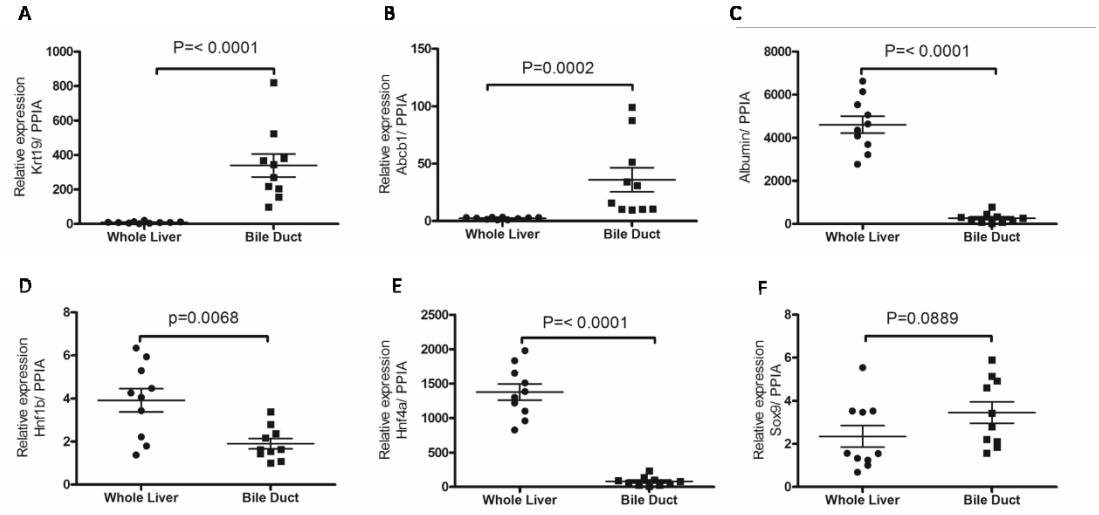

Figure 4.2 QPCR data showing relative expression of key markers of liver and bile duct in whole liver and enriched bile duct samples originating from the same liver, demonstrating enrichment of a biliary population of cells. A, Krt19 relative expression. B, ABCB1 relative expression. C, Albumin relative expression. D, Hnf1β relative expression. E, Hnf4α relative expression. Sox9 relative expression. Data is analysed using the Mann Whitney Test with a 95% confidence interval. $p<0.05$ was deemed to be statistically significant. n=10 biological replicates

4.3 Development a Cholangiocyte Organoid Protocol following enrichment of bile ducts

The isolation of bile ducts from the liver is important for my descriptive work, however to determine functionally what the role of Vangl2 is in bile duct regeneration I decided to establish an in vitro culture of bile duct organoids in which we can modulate the expression of Vangl2.

Following bile duct extraction and enrichment I re-suspended the isolated ducts in Matrigel to provide a three dimensional environment. Matrigel is a combination of laminins, collagen-IV, heparin sulphate proteoglycans and entactin. Rather than using this to form a 2-dimensional polymer base of the tissue culture plastic, I let the Matrigel partially polymerise before plating, as a result the bile ducts are cultured in a raised dome of Matrigel. Bile ducts were cultured with media containing a number of growth factors and small molecule inhibitors. These growth factors fall into distinct classes and are necessary for expansion:

1. Mitogen growth factors, which activate MAPK signaling.

2. Wnt pathway activators, which hyper activate Wnt signaling.

3. TGFβ and ROCK inhibitors that inhibit EMT,

4. Forskolin that potentiates cAMP production

5. Vitamins and amino-acids

The composition of the media can be found in materials and methods. After 24 hours in culture we see the isolated bile ducts close off their open extremities to form capped-off tubules within the matrigel. Expansion of the bile ducts occurs over the following two days, and we see that there are cystic like structures which bud-off the sides and ends of the ducts (Fig.4.3 B,C). These are initially small, but undergo very rapid

expansion after 2 days. After three days the bile ducts are ready to be passaged. The duct like structures are still obvious at this point, however at 3 days they are covered in large, cystic organoids. During passage, organoids are removed from their matrix and are dissociated into fragments by manual disruption and re-embedded in Matrigel. Each fragment will generate a spherical organoid within 24 hours and over the following three days these organoids grow increase in size. After passaging/expanding the population twice more the organoids are significantly cleaner, with the absence of single cells that have carried over from the initial duct isolation. In the space of 7-10 days it is possible to generate a 24 well plate with sufficient organoids for experimentation, this is a significant improvement on previous assays where generation of organoids took a number of months. This method also has the benefit that we can isolate organoids form transgenic animal livers as well as wild-type tissue.

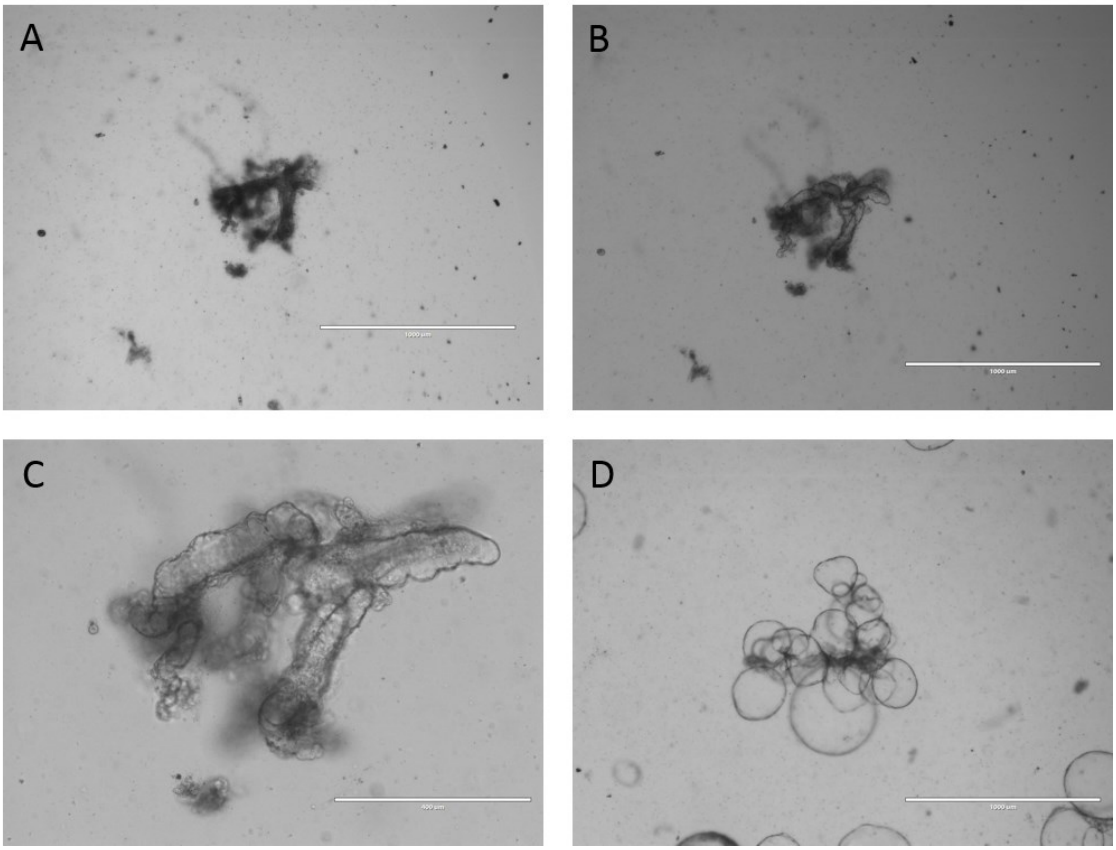

Figure 4.3 Progression of Organoid growth and development. A, Bile duct at day 0. B, Bile duct at day 1. C Bile duct at day 2. D Organoids at day 7 after first passage. Scale bar is 400µm in A,B and D. Scale bar is 1000µm in C.

4.4 Summary of Bile duct enrichment and Validation

In this chapter, I have shown how I developed a methodology in the lab to isolate and culture bile duct organoids. The importance of enriching for our cell population of interest is central as it only makes up 20% of the adult liver and therefore the confounding background in this type of analysis would be difficult to overcome, particularly as I am investigating changes in lowly expressed proteins. I have refined a duct extraction protocol to not only be faster and more efficient but that can deliver ducts that are capable of going on to generate organoids at a faster rate. I successfully validated the duct enrichment by showing a significant difference in key markers of both bile duct and whole liver. In particular, the use of Krt19 and ABCB1 as bile duct markers and albumin and HNF4α as a measure of whole liver or hepatocyte population clearly supports this. Finally, I successfully established a bile duct organoid protocol that is efficient and can be consistently carried out. These organoids will be used in my project and more generally by the lab to look at the functional role of signals in bile duct regeneration and cancer and therefore constitute an important tool for studying these processes.

Chapter 5 – Characterisation of Vangl2 and Non-Canonical Wnt Pathway Components in the Regenerating Bile Duct

Whilst the role of Vangl2 and non-canonical Wnt signaling has been functionally determined during embryogenesis using a combination of genetics from patients with neural tube closure defects and animal models, the function of Vangl2 and non-canonical Wnt signaling in adult tissues remains largely undetermined with work largely being limited to muscle, epidermis and cancers.

5.1 DDC Model

The 3,5-diethoxycarbonyl-1,4-dihydrocollidine (DDC) model was selected as a non-oncogenic model of primary sclerosing cholangitis. The DDC model is a consistently applicable and recognised method of drug-induced cholestatic liver injury in the mouse. Mice tolerated the diet for up to 14 days, with additional experimental time points at days 5, 10 and 14, at which point they were sacrificed.

5.2 QPCR for Non-Canonical Wnt Pathway Components

Using tissue challenged by the DDC diet at 5 days, 10 days and 14 days and compared against uninjured tissue I investigated known receptors and their cited corresponding ligands (Niehrs, 2012).

During the experimental period, I found a significant upregulation Vangl2 (Fig.5.1A) at all three time points when compared to the uninjured day 0 tissue (Vangl2, P=0.0006). There was no significant change found in Vangl1 expression (Fig.5.1B) (Vangl1, P=0.1306).

Of particular interest in this data is the remarkable upregulation at 5 days of DDC injury where Vangl2 is transcriptionally expressed at a mean of ~15-fold increase and Vangl1 is over 5 fold increased. The transcriptional upregulation also takes places at 10 days and 14 days but is most strongly increased at 5 days.

Ror2, a commonly associated Vangl2 and non-canonical Wnt co-receptor was not found the change during the injury period (p=0.595) (Fig.5.1C).

I examined Wnt4 (Fig.5.1E), Wnt5a (Fig.5.1D) and Wnt11 (Fig.5.1F) as archetypal non-canonical pathway markers. Wnt11 showed evidence of change during the DDC injury progression (p=0.0231) (Fig.5.1F) by overall analysis with its greatest relative fold change at day 14. However, there was no change at day 5 or 10 and so it was not initially considered as a candidate ligand. Wnt4 showed a significant increase at 5 days (p=0.0107) (Fig.5.1E) but a drop in expression at 10 days and 14 days when compared against uninjured tissue. We had considered that Wnt4 could be an interesting candidate given it has previously been described as antagonistic to the canonical Wnt signaling pathway (Bernard P et al 2009), and our lab has previously shown that the canonical signal is not activated during bile duct regeneration (Boulter et al 2013). In fact, it is suggested that the non-canonical Wnt pathway is actively inhibited by activated components of the non-canonical pathway featured in this case. Wnt5a mRNA expression is significantly upregulated at all time points (p=0.008) (Fig.5.1D), once again, as previously mentioned when referring to pathway receptors I found a particularly strong increase in expression at 5 days of injury.

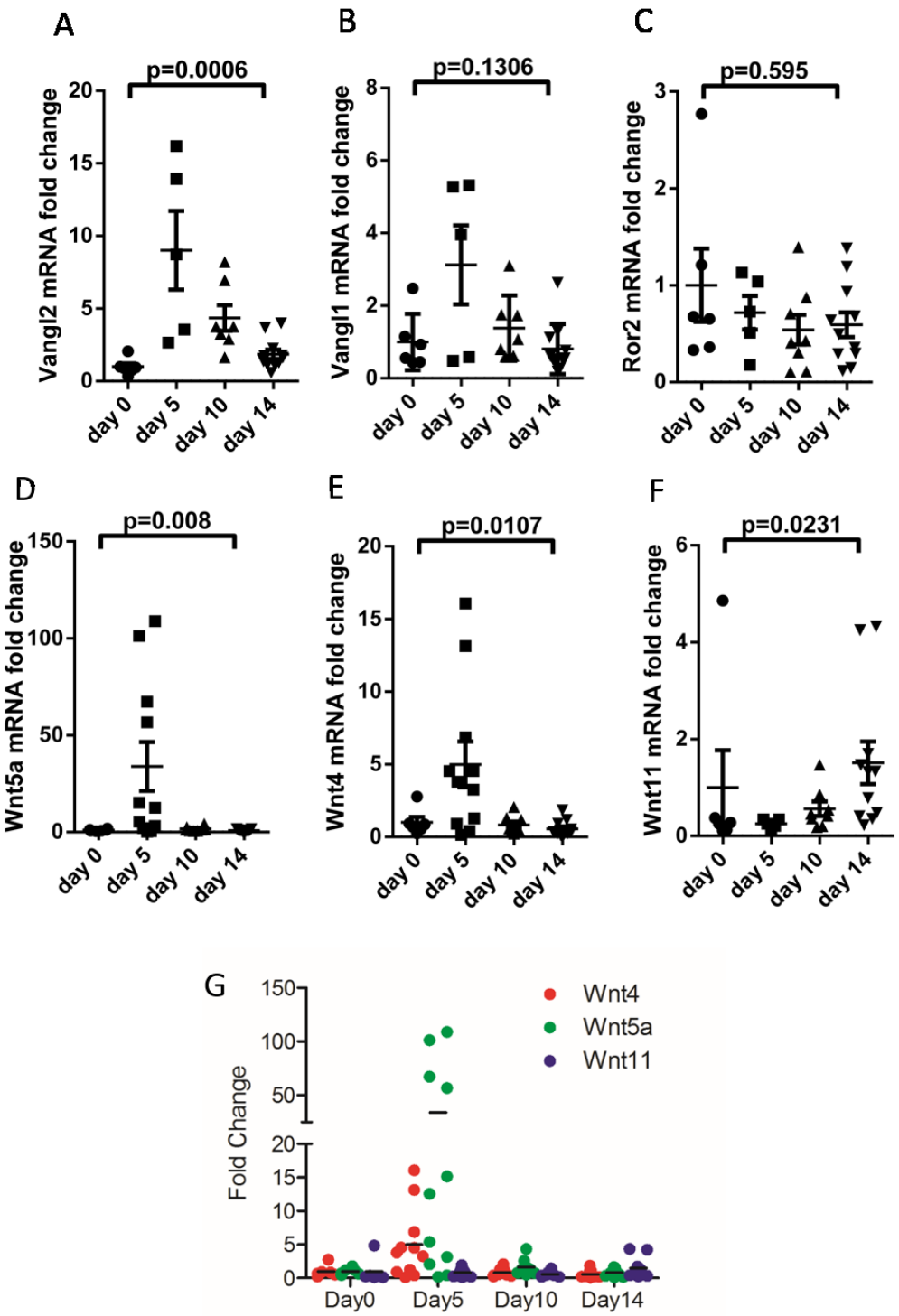

Figure 5.1 qPCR data showing fold change of candidate pathway ligand, receptor and co-receptors transcription. A, Vangl2 mRNA fold change. B, Vangl1 mRNA fold change. C, Ror2 mRNA fold change. D, Wnt5a mRNA fold change. E, Wnt4 mRNA fold change. F, Wnt11 mRNA fold change. G, Combined mRNA fold change for Wnt4a, Wnt5a and Wnt11. Data is analysed using the Kruskal-Wallis Test with a 95% confidence interval. $p<0.05$ was deemed to be statistically significant. n=6

Frizzled (Fzd) is a G protein-coupled receptor that acts as the Wnt receptor in Wnt signaling. There are 10 known Frizzled receptors. The cysteine rich domain of the receptor interacts with Wnts but is not unique to Fzds as it also exists on other known receptors such as Ror2.

The interactions of Wnt ligands with corresponding Fzd receptors is complex but we can narrow down potential receptors that may be being expressed in this case. I assayed for Fzd receptors which are known to function in the non-canonical pathway; Fzd3, Fzd6 and Fzd8 as well as candidate Fzds which are known to function in the canonical pathway. Wnts reported to activate Fzd1 include Wnt1, Wnt8, Wnt3a, Wnt3, and Wnt2. Wnt5a apparently interacts with Fzd1 but does not signal. The only reported Wnt to interact with Fzd2 is Wnt5a.Wnt1 and Wnt8 are reported to bind to Fzd3. Wnts believed to bind to Fzd4 include Wnt1 Wnt8, and possibly, Wnt5a.Wnts reported to bind to Fzd7 include Wnt5a, Wnt8, and Wnt11. Wnt8 is believed to be a ligand for Fzd8.

Conclusive data showed significant upregulation in transcription of Fzd3 (P=0.006) (Fig.5.2C), Fzd4 (p=0.0064) (Fig.5.2D) and Fzd8 (p=0.008) (Fig.5.2G). As with the Wnt ligands I found significant upregulation at all time points but particularly at day 5 during injury, Fzd3 in particular demonstrated a mean 15-fold change in mRNA transcription (Fig.5.2C).

However, as in the case of Ror2, Fzd is not always the Wnt receptor activating the pathway. It would be encompassing to investigate other receptor tyrosine-kinases that reportedly operate in a similar fashion to Ror2, particularly given my data for Ptk7 expression (Fig.5.3E and Fig.5.5). Other RTK's such as Ror1 and Ryk could also be upregulated.

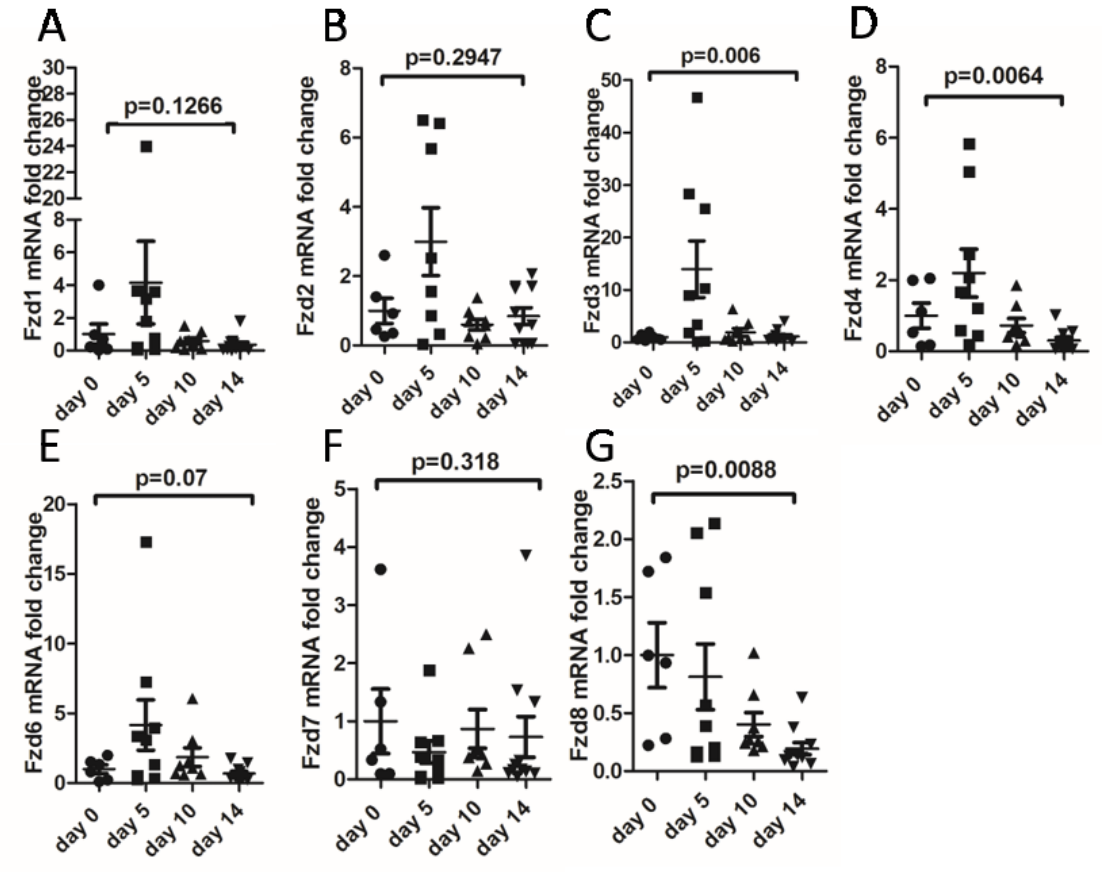

Figure 5.2 qPCR data showing fold change of candidate pathway receptor transcription. A, Fzd1 mRNA fold change. B, Fzd2 mRNA fold change. C, Fzd3 mRNA fold change. D, Fzd4 mRNA fold change. E, Fzd6 mRNA fold change. F, Fzd7 mRNA fold change. G, Fzd8 mRNA fold change. Data is analysed using the Kruskal-Wallis Test with a 95% confidence interval. $p<0.05$ was deemed to be statistically significant. n=6

Disheveled (Dvl) proteins are a family of proteins involved in the canonical and non-canonical Wnt signaling pathways. Historically, Dvl's roles are closely linked to that of the canonical Wnt pathways but also plays an important role in cellular differentiation and cell polarity. In the canonical Wnt signaling pathway, Dvl is phosphorylated where it polymerises and sequesters Axin at the cell membrane by the activation of Fzd by Wnt rendering B-catenin free of the destruction complex and activating the canonical Wnt signaling pathway. There are three evolutionary conserved murine forms Dvl1, Dvl2 and Dvl3.

I examined at the transcription of Disheveled to investigated downstream activation of the Wnt pathway. I found no change in Dvl2 during bile duct injury (p=0.6489) (Fig.5.3B). However, both Dvl1 and Dvl3 were upregulated across the injury time course (Dvl1, P=0.0383 (Fig.5.3A). Dvl3, p=0.011 (Fig.5.3C)). Once again, significant upregulation of mRNA transcription was found at all time points during injury but particularly high transcriptional fold change was found to be occurring at day 5, a feature noted in Vangl2 expression and some Wnt ligands.

To investigate further possibilities of a co-receptor being present I investigated Ryk and Ptk7 expression. Ryk is a known non-canonical Wnt pathway co-receptor that binds with Wnt and directly activates Dvl. It was found to be significantly upregulated at all time points during injury (p=0.021) (Fig.5.3D) but particularly at day 5 exhibiting a 5-fold increase. Ptk7 is a transmembrane pseudokinase known for its role as a regulator of the Wnt mediated planar cell polarity pathway. I found it to be significantly upregulated during the injury time course (p=0.0192) (Fig.5.3E) with an increase in relative transcription over the course of injury.

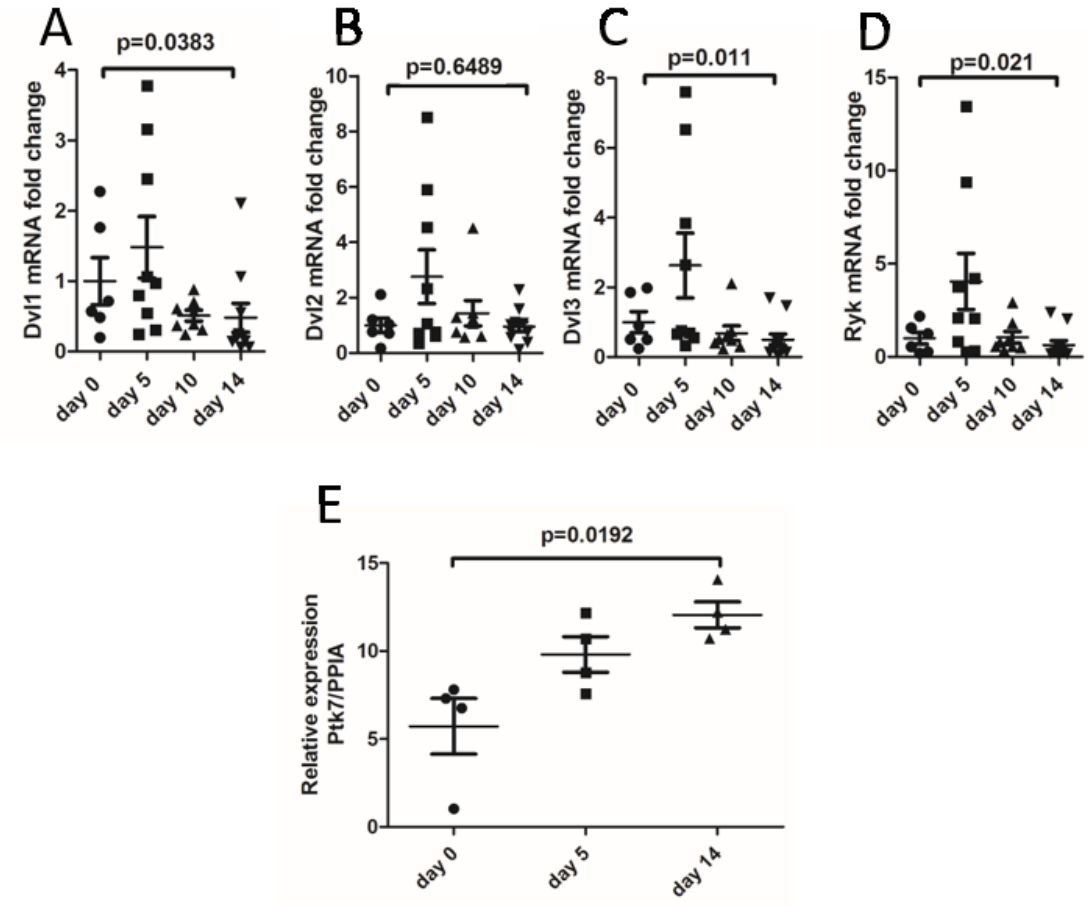

Figure 5.3 qPCR data showing fold change of Disheveled and Ryk co-receptor. A, Dvl1 mRNA fold change. B, Dvl2 mRNA fold change. C, Dvl3 mRNA fold change. D, Ryk mRNA fold change. E, Ptk7 Relative Expression. Data is analysed using the Kruskal-Wallis Test with a 95% confidence interval. $p<0.05$ was deemed to be statistically significant. n=6

5.3 *In Situ* Hybridisation for Vangl1 and Vangl2

With data strongly supporting the hypothesis that Vangl2 and the non-canonical Wnt pathway are involved in the regenerating bile duct I wanted to clarify the location of the upregulated mRNA transcription. I did this by *in situ* hybridisation, probing for Vangl2 mRNA in regenerating tissue from the DDC injury model. I found positive signals for the mRNA in the bile duct epithelium with what looks to be an increased expression of signal as the DDC injury model progressed (Fig.5.4). This is subjective though, this data would need to be quantified and normalise against epithelium number to conclude an increase or not in signal expression.

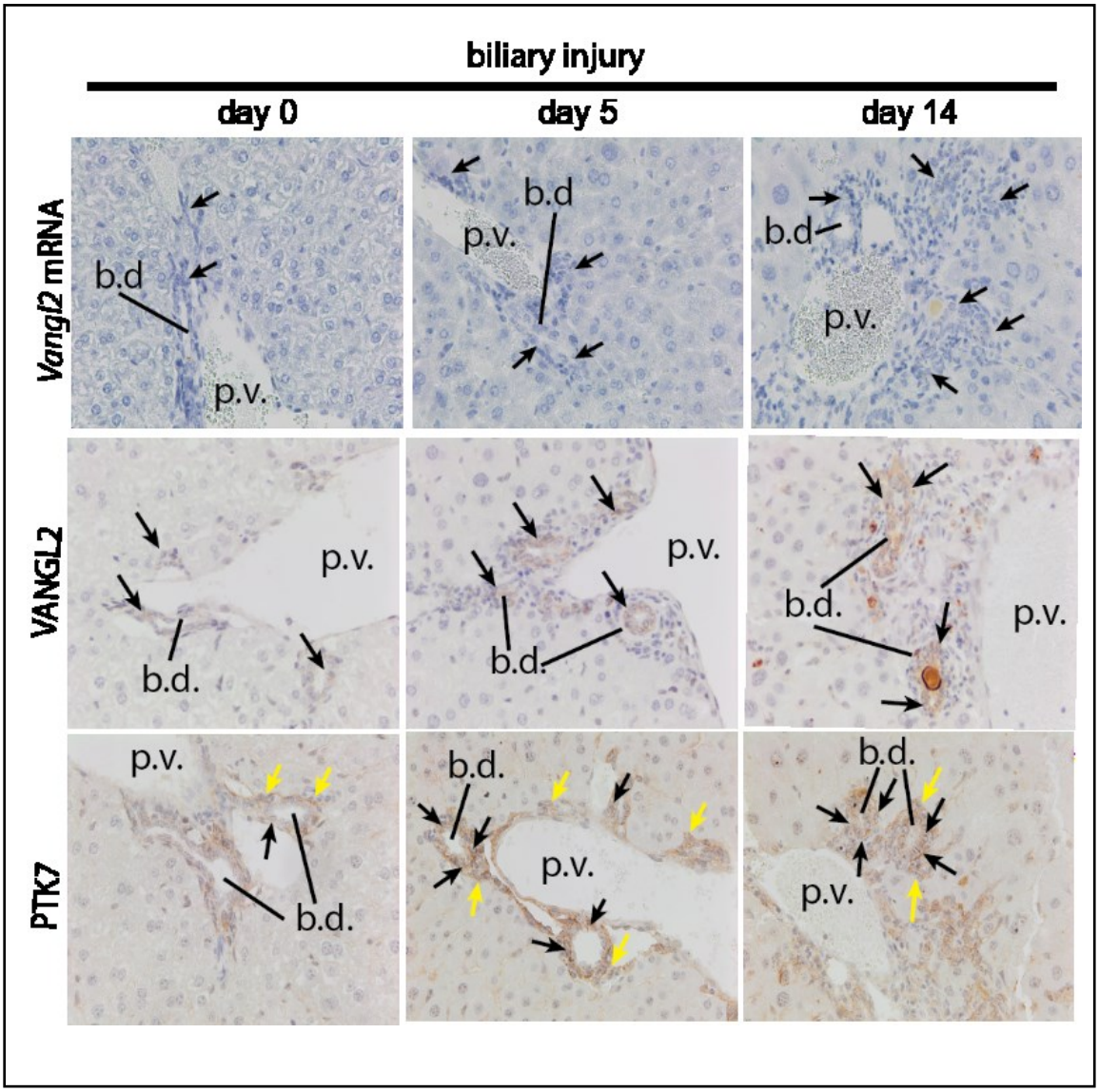

Figure 5.4 Upper panels *In Situ* Hybridisation by RNAScope showing Vangl2 mRNA expression, highlighted by arrows, with spatial localisation of the Bile Duct (b.d.) and Portal vein (p.v.) during DDC injury at days 0, 5 and 14. Immunohistochemistry demonstrating presence and localisation of Vangl2 middle panels and Ptk7 lower panels during bile duct injury

5.4 Vangl2 and Ptk7 protein expression during injury

Dual stained immunofluorescent staining of Vangl2 and PTK7 reveals potential co-localisation of the two receptors, proposing a role for PTK7 interacting with Vangl2 in receiving a Wnt ligand during regeneration of the bile duct (Fig.5.5).

I also examined at Vangl2 expression by immunohistochemistry over the injury process finding increased expression as injury progressed. Unlike the qPCR data I did not see such high expression at day 5 that then receded, instead I saw a steady increase in expression as the time course progressed (Fig.5.5). This may be because the pathway is activated in response to injury at which point it drives Vangl2 expression to ensure a complete response against the expected ligand. Once Vangl2 is translated from mRNA it is expressed on the cell surface but we have no data on the half-life of the receptor expression, perhaps it is expressed there for some time relative to the injury progression? The transcriptional response may also be appropriate for the ligand expression and regenerative purpose. Once the initial response resulting in high Vangl2 expression is achieved the system may only require minimal expression, in comparison to early expression, to maintain the desired response. Vangl2 expression was localised to the vicinity surrounding the bile duct.

Ptk7 showed a similar pattern of expression to that of Vangl2 with increased expression as injury progressed and localisation to the bile duct (Fig.5.5). Of interest, PTK7 is also expressed in the fibroblasts surrounding the Vangl2 positive epithelium, prior to the epithelium expressing PTK7. This suggests that the fibroblasts surrounding the duct may utilise PTK7 independent of Vangl2 to regulate their function, however further experiments would be needed to test this hypothesis.

I did immunofluorescence to look for instances of co-localisation of Vangl2 and PTK7. Under confocal microscopy the expression of both proteins looks consistent with what we would expect should they be expressed in the same regions but of course there are still limitations to truly explore this hypothesis. Ideally, to investigate this would require at least two techniques. I would utilise a co-immunoprecipitation approach to confirm molecular interaction with both proteins. This would not demonstrate localisation but would confirm the possibility of both receptors existing within a bound state. I could then build on this using Fluorescence Resonant Energy Transfer (FRET). In a FRET experiment the potential binding partners are labelled with spectrally distinct fluorophores in such a way that the emission spectrum of the donor molecule overlaps the excitation spectrum of the acceptor molecule. If both interaction partners are in close contact at a distance of only a few nanometers, the excited donor can transfer its energy to the acceptor. In turn, the acceptor emits a fluorescence photon and the fluorescence lifetime of the donor molecule decreases. This demonstrates a relative co-localisation within a given distance. The combination of co-IP and FRET analysis, if successful, would strongly indicate a co-localised interaction.

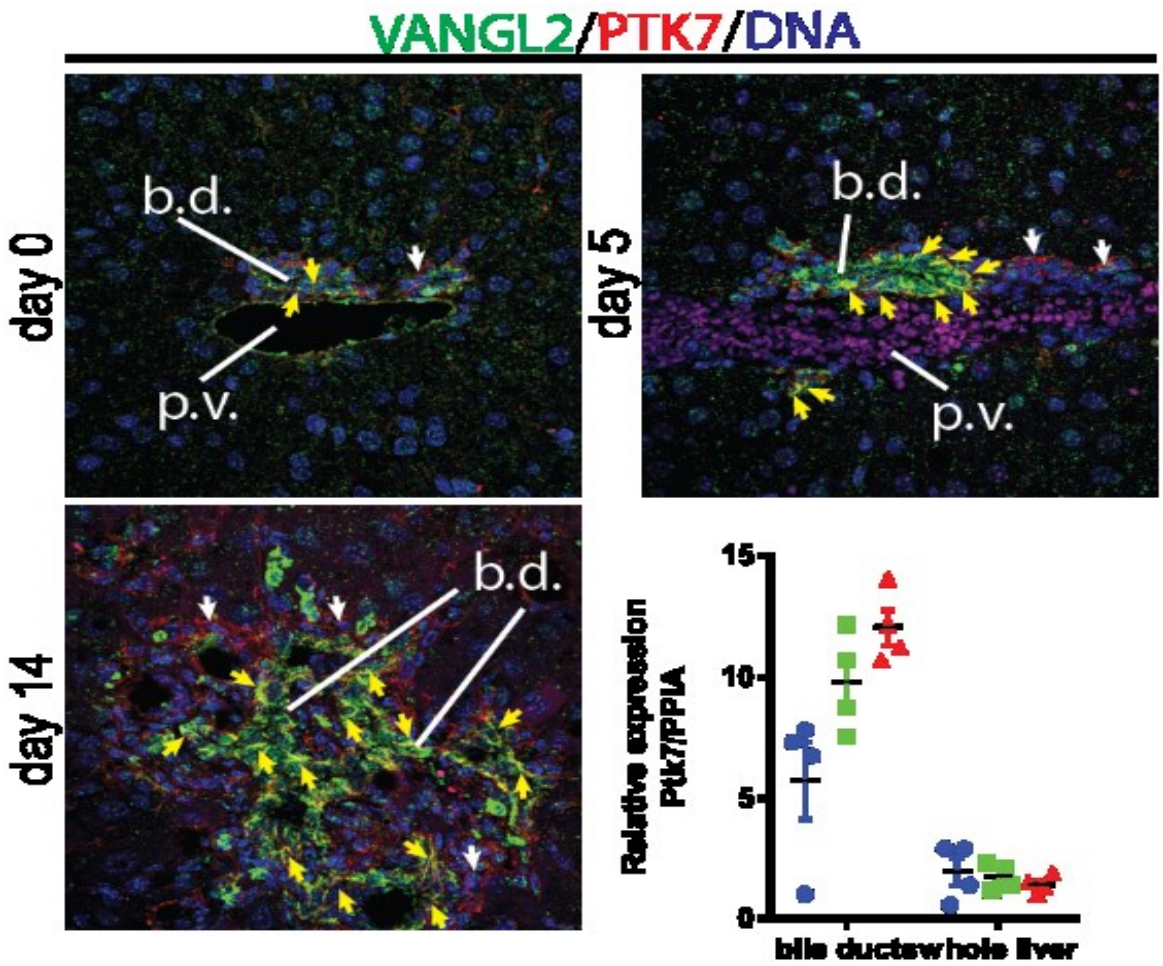

Figure 5.5 Immunofluorescence of dual stained tissue during DDC injury at day 0, 5 and 14 showing Vangl2 in green, Ptk7 in red and nuclear DNA in blue. Yellow signal demonstrates co-localisation of green and yellow signals of Vangl2 and Ptk7. These instances are highlighted by arrows. Bile Ducts (b.d.) are indicated for reference.

5.5 Identification of Vangl2 in Human bile ducts

Previous work from our group has shown that in cholangiocarcinoma, a cancer of the intrahepatic bile ducts, Vangl2 is over expressed at the mRNA level in cancer compared to uninvolved human tissue. To determine whether Vangl2 is expressed in normal and diseased human liver, we identified material from patients who had a diagnosis of PSC versus patients who had a normal liver pathology.

Patient matched samples of PSC and healthy tissue from the same patient were investigated for evidence of Vangl2 transcriptional upregulation and protein expression. I found, using qRT-PCR, that there was a significant up regulation of Vangl2 mRNA transcript ($P=0.023$) (Fig.5.6B) when compared to non-disease tissue. However, the same was not the case when Vangl1 expression was investigated, no significant difference was found between PSC and normal tissue ($p=0.143$) (Fig.5.6A). Whilst qRT-PCR is useful to determine whether Vangl2 is expressed, it does not provide any information about where transcripts or proteins are expressed within the tissue. To better understand this, I used immunohistochemical staining using anti-Vangl1 and anti-Vangl2 antibodies that I have optimised during my MScR. I found that for both Vangl1 and Vangl2 proteins are localised to the biliary epithelium in both normal and PSC tissue (Fig.5.6C). Whilst immunohistochemistry is useful for identification of protein localisation it does not tell us about the levels of Vangl2 protein in the bile ducts. To do this I would need to isolate bile ducts from both normal and PSC tissue and use a quantitative method to determine the levels of Vangl1 and Vangl2 protein in these samples using Western blotting. Given these samples are derived from the NHS ACCORD tissue bank, and are formalin fixed this was not possible from the samples we had available.

Vangl2 is a transmembrane protein, which is known to interact with a number of Wnt ligands via other co-receptors. We had determined in our mouse model of PSC, the DDC diet, that Wnt4 and Wnt5a were significantly over expressed compared to baseline, and could show that Wnt5a was expressed in CD68 positive inflammatory cells using immunohistochemistry. To confirm this in the context of human disease, I investigated whether the ligand for Vangl2 was indeed, Wnt5a, and found a significant up regulation of its transcript ($p=0.024$) (Fig.5.6D) and I could also find small cells which expressed Wnt5a protein by immunohistochemical staining (Fig.5.6E). These cells were localised in the vicinity of the bile duct, however were not bile duct epithelium and are likely to be inflammatory cells. To confirm this, I would need to stain PSC and normal tissue with both WNT5A and CD68 to confirm co-localisation.

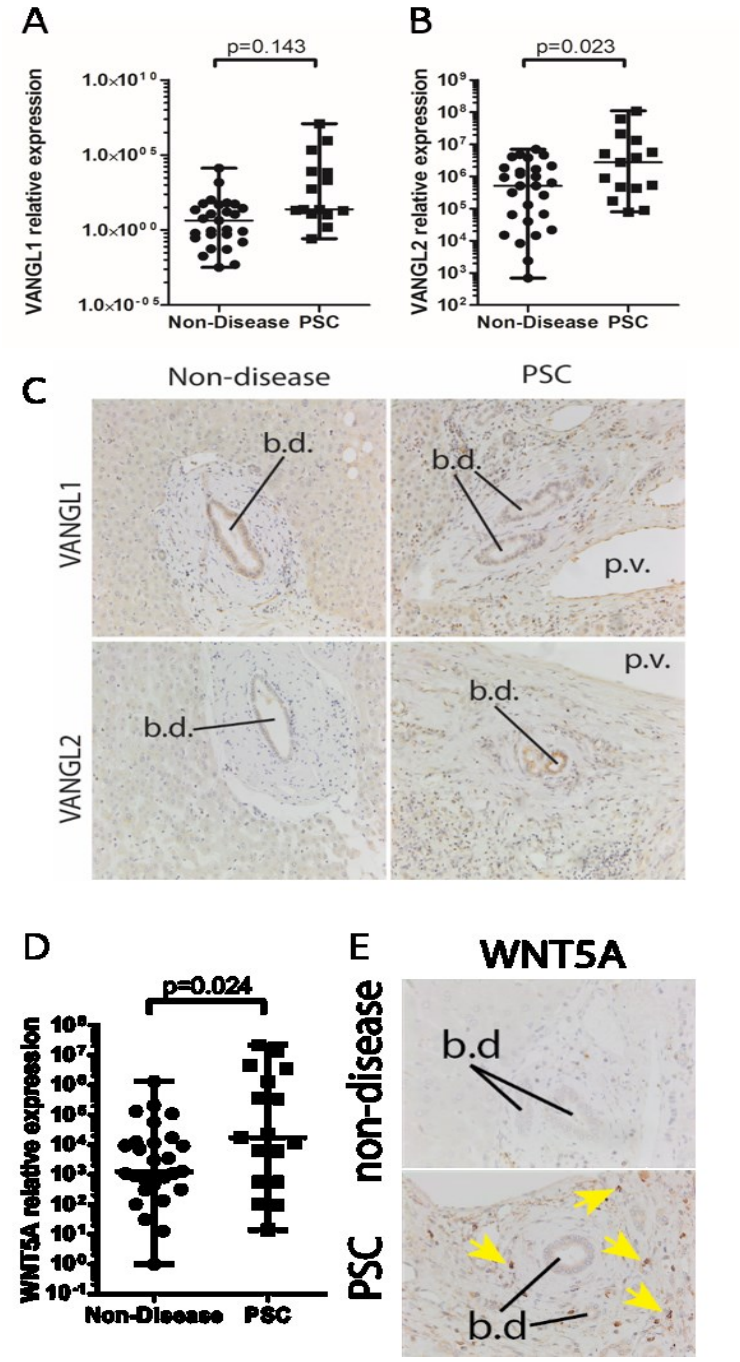

Figure 5.6 Identification of Vangl2 in hCCA. A Vangl1 relative expression. B Vangl2 relative expression. C Immunohistochemistry showing Vangl1 and Vangl2 protein expression with Bile Duct (b.d.) and Portal Vein (p.v.) highlighted. D Wnt5a relative expression. E Immunohistochemistry showing Wnt5a protein expression with Bile Duct (b.d.) highlighted. For RT-qPCR the data is analysed using the Mann Whitney Test with a 95% confidence interval. $p<0.05$ was deemed to be statistically significant. n=17

5.6 Summary of qPCR and immunohistochemistry for non-canonical Wnt Pathway Components during bile duct injury

Here I show strong evidence for the transcriptional upregulation of key components of the non-canonical Wnt pathway during bile duct injury and validate some of this data by *In Situ* hybridisation and immunohistochemistry to show the presence of the protein.

I initially looked for evidence of an archetypal receptor ligand complex. I found strong upregulation of Vangl2, Wnt5a, Wnt4, Fzd3, Fzd4 and Fzd8. Vangl2 mRNA was localised to the bile duct epithelia by RNAScope *In Situ* hybridisation and immunohistochemistry.

I highlighted the activation of a membrane bound Wnt pathway receptor by looking for evidence of Dvl transcription, finding Dvl1 and Dvl3 both upregulated.

I found evidence suggesting a role for PTK7 as a co-receptor by showing increased transcriptional expression as well as immunohistochemistry. The immunohistochemistry hinted at co-localisation with Vangl2 but this will need further work to elucidate.

Finally, I used human samples of Primary Sclerosing Cholangitis to show potential translation of this data to human disease.

Chapter 6 - Modulation of Vangl2 using the Looptail mutation

6.1 Characterisation of the Looptail mutation.

Looptail mice feature a missense point mutation converting a serine to and argenine (S464N) (Fig.6.1A). Vangl2 is transcribed correctly and translocated to the nucleus but fails to function as a transmembrane receptor. The mutation operates in a semi-dominant fashion over the wild-type locus; heterozygotes display the looped-tail appearance while homozygotes show the neural tube defect craniorachishisis in which it fails to close during development. Therefore all experiments are conducted with $Vangl2^{+/+}$ and $Vangl2^{Lp/+}$. The obvious looped or kinked tail is a clear visual marker of phenotype; the mutation also contributes to perturbed cilia function in the inner ear canal. This is demonstrated by poor balance and coordination and a characteristic head tremor.

To confirm the transcriptional activity of Vangl1 and Vangl2 I conducted qPCR. The S464N mutation causes no issue in transcription of mRNA or the translation of protein. The Looptail mutation disrupts delivery of Vangl1 and Vangl2 proteins to the cell surface as a result of oligomer formation between Vangl1 and $Vangl2^{S464N}$, or Vangl2 and $Vangl2^{S464N}$, coupled to the intracellular retention of $Vangl2^{S464N}$. As a result, Vangl1 protein is missing from the apical cell surface of vestibular hair cells in *Looptail* mutants, but is retained at the apical cell surface of hair cells in *vangl2* knockouts. As expected I saw no change in mRNA relative expression (Vangl1, p=0.7247) (Fig.6.1B). Vangl2, p=0.7424) (Fig.6.1C). A number of descriptions have also indicated that Vangl2 can traffic normally to the plasma membrane in certain cells where it functions as a functionally dead receptor.

I investigated the protein expression of Vangl2 during injury using our DDC model with time points at 5 and 14 days. No difference was noted in expression between the

Vangl2$^{+/+}$ and Vangl2$^{Lp/+}$ phenotypes (Fig.6.2). This is unsurprising as Vangl2 is non-functional as a receptor due to the point mutation but still retains the epitope recognised by the Vangl2 antibody used. The protein is translated as normal and a non-functional form expressed at the cell surface.

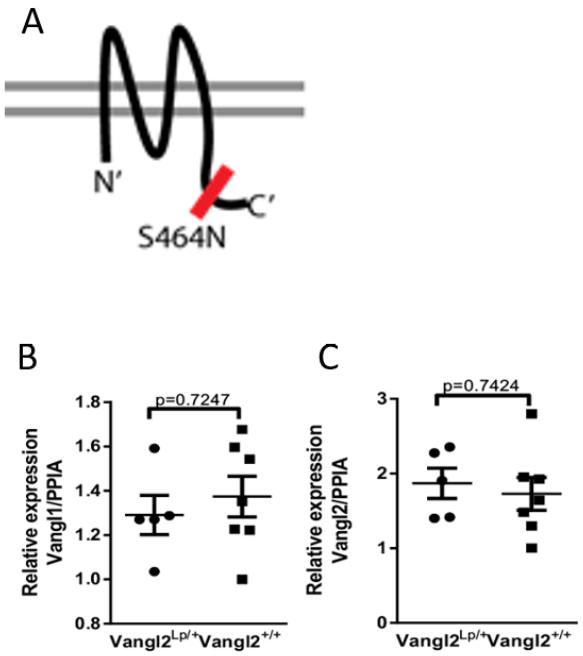

Figure 6.1 A, a schematic showing the C-terminus point mutation featured in the Looptail mouse. B, Vangl1 relative expression in the Looptail and wildtype mouse. C, Vangl2 relative expression in the Looptail and wildtype mouse. qPCR data is analysed using the Mann Whitney Test with a 95% confidence interval. $p<0.05$ was deemed to be statistically significant. n=5

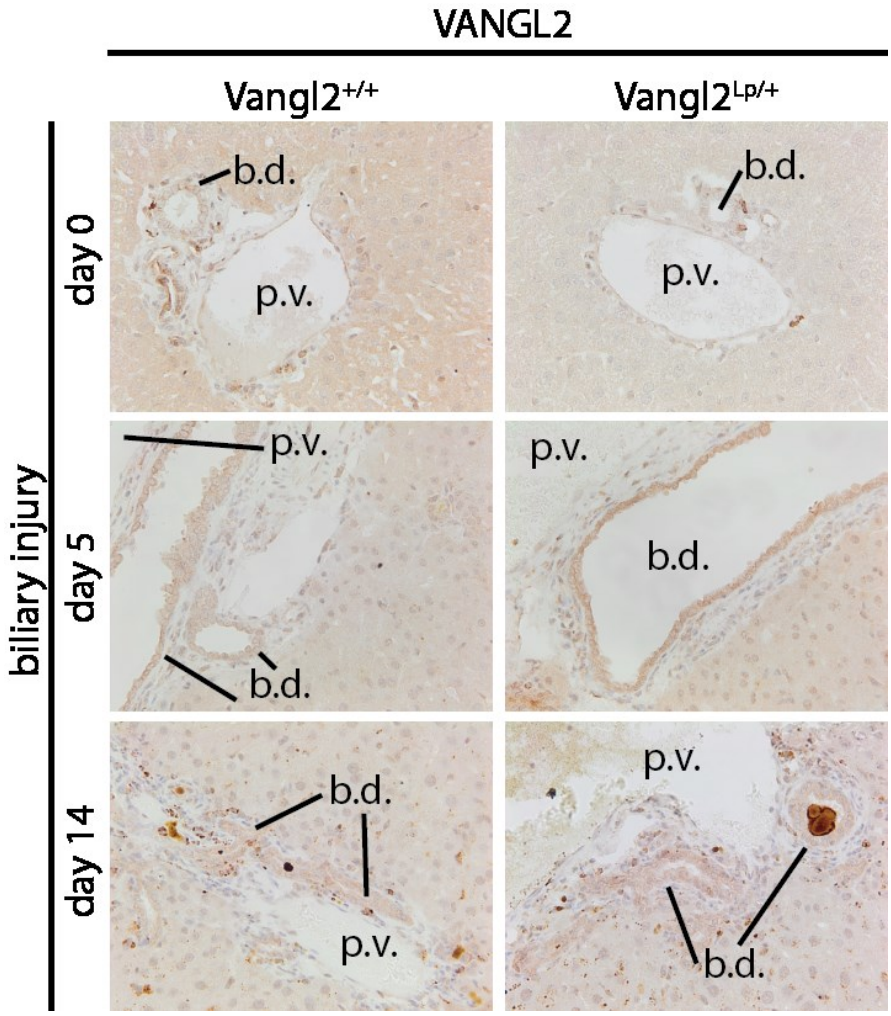

Figure 6.2 Immunohistochemistry demonstrating Vangl2 protein expression in the Wildtype and Looptail mouse at days 0, 5 and 14 during biliary injury by DDC. Bile Ducts (b.d.) and Portal veins (p.v.) are highlighted for reference.

6.2 Characterisation of DDC injury in Vangl2$^{Lp/+}$ mice

I used a Picro-Sirius Red histology stain as an indicator of fibrosis and measured this at day 0 day 5 and day 14 (Fig.6.3E). Sirius Red stains all collagen fibers. I used ImageJ to quantify the area of tissue with positive staining and compared this against to the total area of tissue. I found in both genotypes, Vangl2$^{+/+}$ and Vangl2$^{Lp/+}$ an increase in fibrosis. However, at each time point during injury the Looptail mouse Vangl2$^{Lp/+}$ was found to have significantly less fibrosis than its comparable littermate wildtype (Day 5, p=0.034. Day 14 p=0.002) (Fig.6.3A). I investigated whether this was reduced expression in a specific isoform of collagen within the fibrilar tissue (Fig.6.3F). I found no change in Collagen-III (data not shown) but Collagen-I yielded significant changes. As seen in the analysis of overall fibrosis both genotypes, Vangl2$^{+/+}$ and Vangl2$^{Lp/+}$, showed an increase in Collagen-I during injury. However, at each time point the Looptail mouse Vangl2$^{Lp/+}$ was found to have significantly less fibrosis than its comparable littermate wildtype (Day 5, p=0.030. Day 14 p=0.002) (Fig.6.3B).

I investigated the cell populations that contribute to the fibrogenic response during injury to ascertain whether the populations themselves were increasing resulting in an increase in fibrosis. While the cellular populations do increase during injury ductular fibroblasts (αSMA+) (Fig.6.3C and Fig.6.3G) and stellate cells (Desmin+) (Fig.6.3D and Fig.6.3H) remain unchanged throughout the time course when comparing Vangl2$^{+/+}$ and Vangl2$^{Lp/+}$. A possible hypothesis is that rather than altering the number of fibrogenic cells within the liver, the fibrogenic capacity of these cells is being regulated by Vangl2. Alternatively, Vangl2 is playing a role involved in trafficking MMP14 to the cells surface as part of the fibrogenic response in extra cellular matrix deposition (B. B. Williams et al., 2012), however I would need to formally validate this hypothesis.

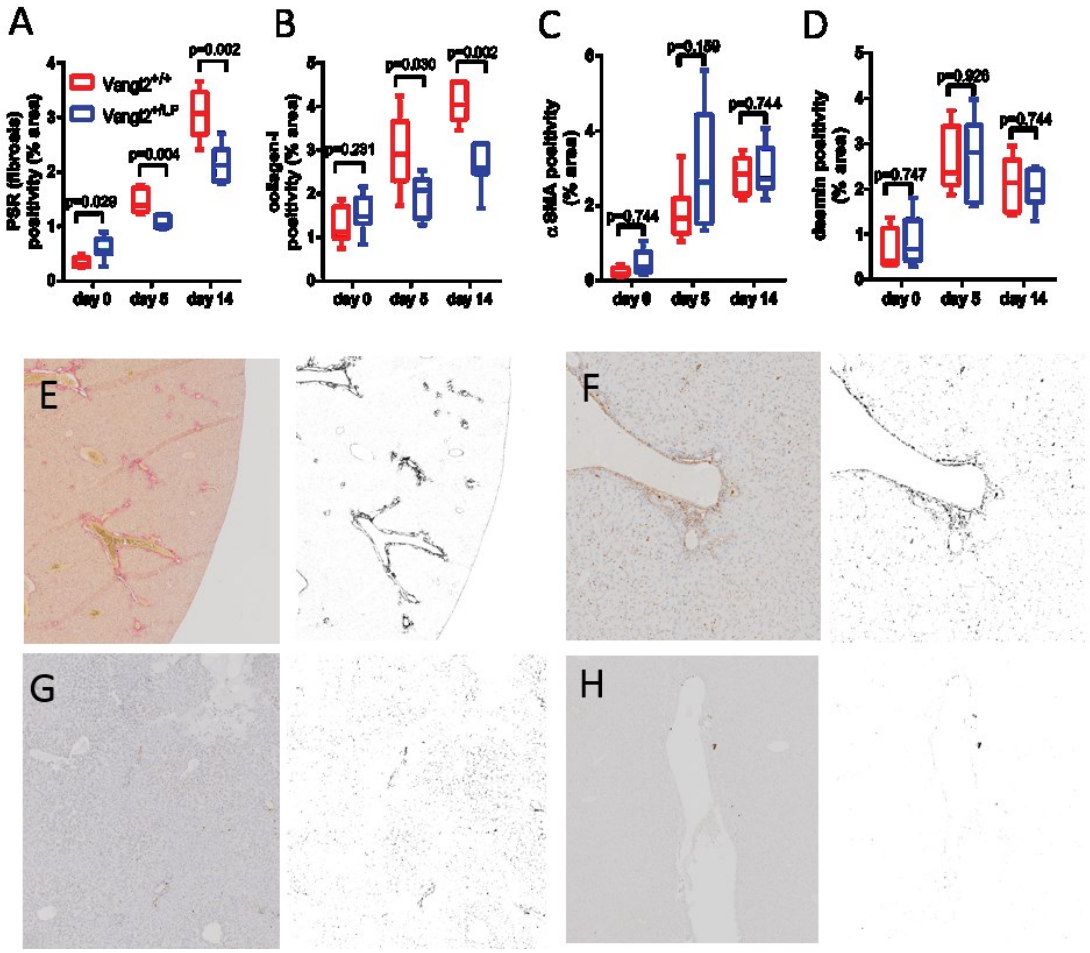

Figure 6.3 Analysis of aspects of fibrosis and contributing cell populations in Looptail mice. A, Quantification of positive PSR staining in Looptail and Wildtype mice during DDC injury. B, Quantification of positive Collagen-I staining in Looptail and Wildtype mice during DDC injury. C, Quantification of positive α-SMA staining in Looptail and Wildtype mice during DDC injury. D, Quantification of positive Desmin staining in Looptail and Wildtype mice during DDC injury. Data is analysed using the Mann Whitney Test with a 95% confidence interval. $p<0.05$ was deemed to be statistically significant. n=5. E, Representative image showing PSR staining and threshold mask of day14 Looptail liver. F, Representative image showing Collagen-1 staining and threshold mask of day14 Looptail liver. G, Representative image showing α-SMA staining and threshold mask of day14 Looptail liver. H, Representative image showing Desmin staining and threshold mask of day14 Looptail liver.

6.3 Summary of Vangl2 modulation

Here I used the Vangl2 heterozygous mutant mouse, referred to as Looptail due to its phenotypic tail which varies from a mild kink to curled, to investigate the cellular response to injury when functional Vangl2 expression is significantly reduced.

I, initially, characterised the Vangl2 present showing that despite the serine to argenine (S464N) mutation Vangl2 was still transcriptionally expressed as normal and that by immunohistochemistry the protein was still trafficked to the cell membrane and presented.

I then investigated the fibrotic and cellular response to injury using our previously DDC model of bile duct injury. I found significantly less fibrotic tissue formed at all injury time points and that this fibrotic tissue was comprised of less Collagen-I when compared to the $Vangl2^{+/+}$ littermates. This brings up a number of avenues which we can explore to investigate the potential link between non-canonical Wnt mediated signaling, regulated by Vangl2, in the liver during bile duct injury and the livers fibrotic response to ductal challenge. I touched on it briefly to look at the cellular populations that would be contributing to fibrogenesis. A decrease in cell population may correspond to the decreased fibrosis found. However, this was hypothesis was not supported and so at the moment I must assume that the fibrogenic capacity of these cells has somehow been influenced by the reduction in functional Vangl2.

Chapter 7 - Discussion

Chronic biliary disease is caused by a number of cholangiopathies including primary biliary sclerosis, primary biliary cholangitis and a number of autoimmune pathologies. Together, these account for a significant, and increasing number of liver disease diagnoses each year. Whilst often considered as end-stage disease pathology these bile duct diseases arise on the background of long-term iterative damage and regeneration, resulting in cycles of inflammation and fibrosis.

In the earliest phases of these diseases, pathology is not established and the formation of a local fibrotic microenvironment around damaged ducts is an attempt to regenerate the diseased epithelium whilst concurrently partitioning off this section of injury from the remainder of the organ to prevent the dissemination of disease throughout the tissue (Ramachandran & Iredale, 2012). Here, prior to established disease, this fibrotic microenvironment is known as the regenerative niche and represents a transient and highly specialised microenvironment through which the bile duct is able to regenerate following injury.

Work from the Boulter lab and others have previously demonstrated that this regenerative microenvironment is comprised of a complex mixture of fibrogenic αSMA positive fibroblasts, macrophages, neutrophils and T-cells (Boulter et al., 2012; Greenbaum & Wells, 2011; Viebahn et al., 2010). This complex microenvironment results in the deposition of extra-cellular matrix (ECM), which consists of collagen-1 and collagen-3, but also contains large amounts of laminin, which is known to have a functional role on the biology of the regenerating bile duct. The cellular components of this regenerative niche are also critical for correct biliary specification and the correct patterning of the regenerating ducts.

One major question that remains regarding ductular regeneration is how does the regenerative microenvironment get recruited and, importantly, how does the damaged epithelium communicate to the surrounding niche to affects its biology, ensuring that scar formation is linear to the level of injury, for example?

The Boulter lab is interested in the role of Wnt signaling in liver regeneration and cancer and had previously shown that Vangl2, a component of the non-canonical Wnt receptor complex was over expressed in bile duct cancer. Given that Vangl2 has been previously implicated in the turnover of ECM in the developing embryo (B Blairanne Williams, Mundell, Dunlap, & Jessen, 2012) we sought to investigate, in adult bile duct disease, whether Vangl2 was involved in ECM deposition or turnover.

Here, we are able to show that the non-canonical Wnt receptor Vangl2 is upregulated in bile duct disease compared to healthy liver. Our initial investigations on whole tissue were positive and led us to define the other non-canonical Wnt co-receptors that are likely to be expressed in bile ducts. Enrichment of the bile ducts is crucial when investigating the relatively small population of cells that comprises these structures and in particular when investigating low levels of transcript as is the case in these signaling pathways. In order to address this limitation of cellular dilution by the parenchyma, I established a protocol through which I could isolate the bile ducts from whole liver, thereby enriching the transcriptional abundance of our targets compared to whole liver. My approach to enrich for the population of cells of interest was wholly successful as demonstrated by the qPCR validation data I obtained identifying recognised ductal markers, K19 and ABCB1 in the suspected enriched fraction. Moreover, we could then test these enriched bile duct samples to confirm whether the non-canonical Wnt receptor Vangl2 and PTK were expressed here, which they were. This is the first description in the adult of

Vangl2 and PTK7 being expressed in the adult bile duct, and is in line with previous evidence from the developing liver in zebrafish that Vangl2 might be important for the formation and indeed regeneration of the bile duct (Cui, Capecci, & Matthews, 2011b; Wilkins & Pack, 2013).

As part of this identification and classification I established a protocol to culture bile ducts in Matrigel and expand these as organoids. This protocol is similar to the protocol established by Huch *et al* (Huch & Koo, 2015). However, through my protocol we can rapidly establish very large numbers of organoids. I had intended to use these organoids to more thoroughly define the sub-cellular localisation of Vangl2 at a single cell level, and this should be work done in the future. The establishment of a biliary organoid protocol will prove to be of great use in the future, particularly as we will be able to modulate the non-canonical signaling pathway through genetic alteration of Vangl2 or ligands such as Wnt5a. It will also provide me with a 3-dimensional model of bile ducts, facilitating wide scale screens and analysis in future projects.

The non-canonical Wnt receptor Vangl2 does not operate independently and I therefore undertook a thorough characterisation of pathway components which, in other systems, have been shown to interact with Vangl2. Using qPCR, I showed that during injury we have a significant upregulation of non-canonical Wnt pathway receptors and ligands. The non-canonical ligands, Wnt4 and Wnt5a showed significant upregulation. Furthermore, GPRCs; Fzd3, Fzd4 and Fzd8 also showed significant transcriptional upregulation during injury progression, suggesting that these receptors could be a part of this receptor complex or could be involved in other signaling processes, such as the Wnt dependant calcium/calmodulin signalling pathway. Despite the transcriptional evidence for Fzd being present I could not achieve conclusive evidence by also demonstrating its presence by

immunohistochemistry or Western blot, which would represent further studies. It would also be important to show that these Fzd receptors physically interact with Vangl2 following stimulation with non-canonical Wnt ligands. To further elucidate the nature of the activated pathway it would be prudent to investigate downstream components that became phosphorylated or activated. I would initially continue exploring the archetypal non-canonical components such as DAAM1, RHOA and ROCK. It would then be rational to evaluate whether G-Actin is being converted to F-Actin following upstream changes. If we were to see cytoskeletal changes taking place, this could represent cell shape changes which could influence the local environment. Alternatively, RAC1 and JNK upregulation and activation might lead to cJUN/cFOS activation and changes in transcriptional activation of target genes, which are known to regulate inflammatory cytokines (Chopra, Kumar, Rangarajan, & Kondaiah, 2015; Pashirzad et al., 2016).

To develop this further, it would be possible to perform RNAseq using the Looptail mouse following the DDC injury model. This would give broad scope insight into pathway activations, from this we would be able to use Gene Ontology (GO) term analysis which would allow us to determine which downstream pathways are changed by the Looptail mutation. Given my data showing that the Looptail mutant mice have reduced fibrosis compared to their non-mutant littermates, we have concluded that Vangl2 is involved in the fibrotic response during injury. However, at the moment we have little information of how this is functioning. Changes in the amount of ECM does not necessarily mean there is a change in the composition of the ECM. By isolating the ECM fraction from Looptail and control mice we would be able to use the tissue to analyse ECM by mass spectrometry, this is something that could lead to a number of interesting leads in future studies. This would clearly allow us to understand as to whether certain components of the ECM are expressed differently during bile duct injury when Vangl2 is mutated.

The Looptail mouse, is a commonly employed tool used to investigate the function of Vangl2 in adult tissues. However, it is limited in some regard as the mutation can only be maintained in the adult as a heterozygote and whilst there is a clear phenotype it is impossible to know whether this represents haploinsufficiency and whether this phenotype can be enhanced by homozygous loss. Moreover, Vangl2 function is affected wherever Vangl2 is expressed and does not target the biliary niche I am looking specifically at in this project. As a result, we cannot say, absolutely, that the phenotype in the Looptail mouse we have described is due to loss of Vangl2 function in the bile ducts, although this is likely it could be due to loss of function in other cells which affect fibrosis or due to systemic changes in the Looptail mutant mouse. A more refined approach would be to use a Cre mediated knockout of Vangl2. To do this I would use Cre recombinase expressed from biliary specific promoter, such as Kertain19, Sox9 or Hnf1β, all of which have been previously described. These mice would then be crossed with a Vangl2-flox line. A suitable existing option would be the $Vangl2^{flox}$ mouse used previously by Henderson *et al* to demonstrate adult corneal epithelial cell alignment and migration and patternation of the second-heart field (Findlay et al., 2016). I would then conduct a repeat of the Looptail experiments using this mouse line specifically lacking biliary Vangl2. I would expect the two genotypes, $Vangl2^{Lp/+}$ and $Vangl2^{flox}$ to phenocopy one another, however mice with the Vangl2 homozygous flox allele could have a more significant phenotype. Given that the Looptail mutation is dominant over the wild-type copy in the Looptail mouse, the changes we see may be very similar to the constitutive mutation.

Whilst there have been a large number of small molecules which have been trialed in both rodent models and human diseases targeted against the canonical Wnt signaling pathway, there are relatively few therapeutics which can be used to inhibit the non-canonical Wnt signaling pathway. One way of antagonising the non-canonical Wnt pathway

would be to affect the expression or production of Wnt ligand or to block the activation of the non-canonical Wnt receptors. The use of LGK974 has been recently described as a small molecule inhibitor of PORCN (Porcupine) to target Wnt-driven cancers (Liu et al., 2013). Porcupine regulates Wnt secretion via the endoplasmic reticulum by mediating the palmitolyation of the Wnt ligands. Inhibition of porcupine prevents the secretion of Wnt from its source cell and results in Wnt ligand accumulating in these cells. I would treat mice with biliary injury with LGK974 to inhibit Wnt ligand production and evaluate whether this is sufficient to reduce the deposition of collagen in vivo.

A further strategy to reduce the amount of Wnt ligand produced in this system would be to inhibit the cell of origin. Macrophage derived Wnt in the liver has been highlighted as playing a role in specifying hepatic progenitor cells and also in liver cancer. Macrophages have been implicated elsewhere as being the source of secreted Wnts (Boulter et al., 2012). Their mobility makes them well suited to translocating to injury sites to deliver highly localised ligands in a damage dependent context. Investigating macrophages as a Wnt source and modulator of fibrosis would be straightforward. Initially, macrophage population would be identified with a known marker like F4/80 or CD68. This would allow for identification of macrophage localisation, which under DDC would be surrounding the bile ducts, as previously described. This could be combined with immunohistochemistry for Wnt4 and Wnt5a, which I have shown, are up regulated in the DDC model. Assuming a correlation in macrophage and Wnt localisation the following step would be macrophage ablation, to remove the suspected source of Wnt during biliary disease. This could be done using compounds such as liposomal clodronate, which would ablate phagocytic macrophages or through inhibiting the CSF1 receptor.

The non-canonical Wnt signaling pathway is poorly described and there is a lack of rigorous functional description of non-canonical Wnt pathway and its role in adult liver disease, compared with its canonical counterpart. This means that there is plenty of scope for novel descriptions and functional characterisation of non-canonical pathway activation and its role in disease. Whilst originally described as a mechanism to ensure polarity of epithelial sheets (Vladar, Antic, & Axelrod, 2009), non-canonical Wnt signaling is now largely accepted to have a much more diverse role, particularly in the adult where confluent morphogenic movements are not required (Freese, Pino, & Pleasure, 2010; Fuerer, Nusse, & Ten Berge, 2008; Roel Nusse & Nusse, 2005).

In this MScR, I have shown that there are non-canonical Wnt pathway components expressed in a model of bile duct disease and regeneration. I propose a novel role for Vangl2 and the non-canonical Wnt mediated pathway. While Vangl2 has been previously described as an effective co-receptor for Frizzled in the case of this body of work I would suggest it is acting either independently or as a co-receptor in companion with Ptk7. Through this complex, the non-canonical Wnt signaling pathway is receiving ligand stimulation, potentially Wnt4 or Wnt5a and activating downstream signaling in a hitherto undescribed manner.

Given the reduction I observe in fibrosis in the Vangl2$^{Lp/+}$ mutant mouse subjected to the DDC injury model, this provides a strong insight into the bile-duct specific activation of the non-canonical Wnt pathway via Vangl2. Recent work by Williams *et al* demonstrated a role for Vangl2 in trafficking MMP14 to facilitate cell polarity and migration (B. B. Williams et al., 2012). Subsequently, the same group described a role for Vangl2 dependent sorting in the late endosome, which regulated the presentation of MMP14 at the cell surface. Mutations in Vangl2 resulted in a failure to endocytose MMP14 and therefore resulted in a

higher concentration of MMP activity at the cell surface. This MMP is also known to activate a number of cytokines, soluble MMPs and also can turn over collagen, indicating that in our model system, loss of Vangl2 could in fact regulate the local microenvironment through deregulation of bile duct MMP14 activity. (B Blairanne Williams et al., 2012).

Finally, I have used fibrosis as a readout of change when Vangl2 is altered in the mutant Vangl2 model. However, it would be interesting to combine this data with physiological sampling such as liver function, which would represent the functional output of the liver which may be altered following deregulation of Vangl2.

Ultimately, I have shown, for the first time that the non-canonical Wnt signaling pathway is expressed in bile duct regeneration and that it represents an attractive therapeutic target to modulate the fibrotic response in the adult liver. There remains a great deal of work to do to properly understand the mechanisms behind this pathway in this disease process, however I have functionally shown that this pathway is important by using a mutant allele of Vangl2 and have surprising demonstrated that this is not due to changes in the bile duct proliferation or patterning, but functions potentially in a cell non-autonomous way to regulate bile duct fibrosis.

References

Amerongen, V., Fuerer, C., Mizutani, M., & Nusse, R. (2012). Wnt5a can both activate and repress Wnt / b -catenin signaling during mouse embryonic development, *369*(1), 1–14. https://doi.org/10.1016/j.ydbio.2012.06.020

Boulter, L., Govaere, O., Bird, T. G., Radulescu, S., Ramachandran, P., Pellicoro, A., … Forbes, S. J. (2012). Macrophage-derived Wnt opposes Notch signaling to specify hepatic progenitor cell fate in chronic liver disease. *Nature Medicine*, *18*(4), 572–9. https://doi.org/10.1038/nm.2667

Chopra, S., Kumar, N., Rangarajan, A., & Kondaiah, P. (2015). Context dependent non canonical WNT signaling mediates activation of fibroblasts by transforming growth factor-β. *Experimental Cell Research*, *334*(2), 246–259. https://doi.org/10.1016/j.yexcr.2015.03.001

Cui, S., Capecci, L. M., & Matthews, R. P. (2011a). Disruption of planar cell polarity activity leads to developmental biliary defects. *Developmental Biology*, *351*(2), 229–41. https://doi.org/10.1016/j.ydbio.2010.12.041

Cui, S., Capecci, L., & Matthews, R. (2011b). Disruption of planar cell polarity activity leads to developmental biliary defects. *Developmental Biology*, *351*(2), 229–41. https://doi.org/10.1016/j.ydbio.2010.12.041

Ding, B.-S., Nolan, D. J., Butler, J. M., James, D., Babazadeh, A. O., Rosenwaks, Z., … Rafii, S. (2010). Inductive angiocrine signals from sinusoidal endothelium are required for liver regeneration. *Nature*, *468*(7321), 310–5. https://doi.org/10.1038/nature09493

Doudney, K., & Stanier, P. (2005). Epithelial cell polarity genes are required for neural tube closure. *American Journal of Medical Genetics. Part C, Seminars in Medical Genetics*, *135C*, 42–47. https://doi.org/10.1002/ajmg.c.30052

Eroschenko, V. P. (2012). *diFiore's Atlas of Histology with Functional Correlations* (10th ed.).

Fava, G. (2010). Molecular mechanisms of cholangiocarcinoma. *World Journal of Gastrointestinal Pathophysiology*, *1*(1), 12–22. https://doi.org/10.4291/wjgp.v1.i1.12

Fickert, P., Pollheimer, M. J., Beuers, U., Lackner, C., Hirschfield, G., Housset, C., … Trauner, M. (2014). Characterization of animal models for primary sclerosing cholangitis (PSC). *Journal of Hepatology*, *60*(6), 1290–1303. https://doi.org/10.1016/j.jhep.2014.02.006

Fickert, P., Stöger, U., Fuchsbichler, A., Moustafa, T., Marschall, H.-U., Weiglein, A. H., … Trauner, M. (2007). A new xenobiotic-induced mouse model of sclerosing cholangitis and biliary fibrosis. *The American Journal of Pathology*, *171*(2), 525–36. https://doi.org/10.2353/ajpath.2007.061133

Findlay, A. S., Panzica, D. A., Walczysko, P., Holt, A. B., Henderson, D. J., West, J. D., … Collinson, J. M. (2016). The core planar cell polarity gene, *Vangl2* , directs adult corneal epithelial cell alignment and migration. *Royal Society Open Science*, *3*(10), 160658. https://doi.org/10.1098/rsos.160658

Freese, J. L., Pino, D., & Pleasure, S. J. (2010). Wnt signaling in development and disease. *Neurobiology of Disease*, *38*(2), 148–153. https://doi.org/10.1016/j.nbd.2009.09.003

Fuerer, C., Nusse, R., & Ten Berge, D. (2008). Wnt signalling in development and disease. Max Delbrück Center for Molecular Medicine meeting on Wnt signaling in Development and Disease. *EMBO Reports*, *9*(2), 134–138. https://doi.org/10.1038/sj.embor.7401159

Gao, B., Song, H., Bishop, K., Elliot, G., Garrett, L., English, M. A., … Yang, Y. (2011). Wnt signaling gradients establish planar cell polarity by inducing Vangl2 phosphorylation through Ror2. *Developmental Cell*, *20*(2), 163–76. https://doi.org/10.1016/j.devcel.2011.01.001

Glaser, S., & Gaudio, E. (2009). Cholangiocyte proliferation and liver fibrosis. *Expert Reviews in …*, *11*, e7. https://doi.org/10.1017/S1462399409000994

Greenbaum, L. E., & Wells, R. G. (2011). The role of stem cells in liver repair and fibrosis. *The International Journal of Biochemistry & Cell Biology*, *43*(2), 222–9. https://doi.org/10.1016/j.biocel.2009.11.006

Hatakeyama, J., Wald, J. H., Printsev, I., Ho, H.-Y. H., & Carraway, K. L. (2014). Vangl1 and Vangl2: planar cell polarity components with a developing role in cancer. *Endocrine-Related Cancer*, *21*(5), R345-56. https://doi.org/10.1530/ERC-14-0141

Huch, M., & Koo, B.-K. (2015). Modeling mouse and human development using organoid cultures. *Development*, *142*(18), 3113–3125. https://doi.org/10.1242/dev.118570

Katoh, M. (2002). Strabismus (STB)/Vang-like (VANGL) gene family (Review). *International Journal of Molecular Medicine*, *10*(1), 11–5. Retrieved from http://www.ncbi.nlm.nih.gov/pubmed/12060845

Liu, J., Pan, S., Hsieh, M. H., Ng, N., Sun, F., Wang, T., … Harris, J. L. (2013). Targeting Wnt-driven cancer through the inhibition of Porcupine by LGK974. *Proceedings of the National Academy of Sciences of the United States of America*, *110*(50), 20224–9. https://doi.org/10.1073/pnas.1314239110

Macheda, M. L., Sun, W. W., Kugathasan, K., Hogan, B. M., Bower, N. I., Halford, M. M., … Stacker, S. a. (2012). The Wnt receptor Ryk plays a role in mammalian planar cell polarity signaling. *The Journal of Biological Chemistry*, *287*(35), 29312–23. https://doi.org/10.1074/jbc.M112.362681

Martinez, S., Scerbo, P., Giordano, M., Daulat, A. M., Lhoumeau, A.-C., Thome, V., … Borg, J.-P. (2015). The PTK7 and ROR2 receptors interact in the vertebrate WNT/PCP pathway. *Journal of Biological Chemistry*, *290*(51), jbc.M115.697615. https://doi.org/10.1074/jbc.M115.697615

McNeill, H., & Woodgett, J. R. (2010). When pathways collide: collaboration and connivance among signalling proteins in development. *Nature Reviews. Molecular Cell Biology*, *11*(6), 404–13. https://doi.org/10.1038/nrm2902

Mlodzik, M. S. and M. (2010). Planar Cell Polarity Signaling: From Fly Development to Human Disease, (Table 1), 1–29. https://doi.org/10.1146/annurev.genet.42.110807.091432.Planar

Montcouquiol, M., Sans, N., Huss, D., Kach, J., Dickman, J. D., Forge, A., … Kelley, M. W. (2006). Asymmetric localization of Vangl2 and Fz3 indicate novel mechanisms for planar cell polarity in mammals. *The Journal of Neuroscience : The Official Journal of the Society for Neuroscience*, *26*(19), 5265–75. https://doi.org/10.1523/JNEUROSCI.4680-05.2006

Mouri, K., Nishino, Y., Arata, M., Shi, D., Horiuchi, S., & Uemura, T. (2014). A novel planar polarity gene pepsinogen-like regulates wingless expression in a posttranscriptional manner. *Developmental Dynamics : An Official Publication of the American Association of Anatomists*, *243*(6), 791–9. https://doi.org/10.1002/dvdy.24112

Nakanuma, Y. (2012). Tutorial review for understanding of cholangiopathy. *International*

Journal of Hepatology, *2012*, 547840. https://doi.org/10.1155/2012/547840

Niehrs, C. (2012). The complex world of WNT receptor signalling. *Nature Reviews. Molecular Cell Biology*, *13*(12), 767–79. https://doi.org/10.1038/nrm3470

Nusse, R., & Nusse, R. (2005). Wnt signaling in disease and in development. *Cell Research*, *15*(1), 28–32. https://doi.org/10.1038/sj.cr.7290260

Nusse, R., van Ooyen, A., Cox, D., Fung, Y. K., & Varmus, H. Mode of proviral activation of a putative mammary oncogene (int-1) on mouse chromosome 15. *Nature*, *307*(5947), 131–136. https://doi.org/10.1038/307131a0

Pashirzad, M., Shafiee, M., Rahmani, F., Behnam-Rassouli, R., Hoseinkhani, F., Ryzhikov, M., … Hassanian, S. M. (2016). Role of Wnt5a in the Pathogenesis of Inflammatory Diseases. *Journal of Cellular Physiology*. https://doi.org/10.1002/jcp.25687

Ramachandran, P., & Iredale, J. P. (2012). Liver fibrosis: a bidirectional model of fibrogenesis and resolution. *QJM : Monthly Journal of the Association of Physicians*, *105*(9), 813–7. https://doi.org/10.1093/qjmed/hcs069

Stanfield, C. (2012). *Principles of Human Physiology (5th Edition)* (5th ed.).

Stevens, A., & Lowe, J. (1996). *Human Histology* (2nd ed.).

Stöger, U., Fickert, E., Fuchsbichler, A., Moustafa, T., Gumhold, J., Silbert, D., … Trauner, M. (2006). 320 3.5-Diethoxycarbonyl-1.4-dihydrocollidine (DDC) feeding induces cholestasis, chronic inflammatory bile duct damage and biliary fibrosis in mice. *Journal of Hepatology*. https://doi.org/10.1016/S0168-8278(06)80321-1

Takeuchi, M., Nakabayashi, J., Sakaguchi, T., Yamamoto, T. S., Takahashi, H., Takeda, H., & Ueno, N. (2003). The prickle-related gene in vertebrates is essential for gastrulation cell movements. *Current Biology : CB*, *13*(8), 674–9. https://doi.org/10.1016/S

Torban, E., Wang, H.-J., Groulx, N., & Gros, P. (2004). Independent mutations in mouse Vangl2 that cause neural tube defects in looptail mice impair interaction with members of the Dishevelled family. *The Journal of Biological Chemistry*, *279*(50), 52703–13. https://doi.org/10.1074/jbc.M408675200

van Amerongen, R., & Nusse, R. (2009). Towards an integrated view of Wnt signaling in development. *Development (Cambridge, England)*, *136*, 3205–3214. https://doi.org/10.1242/dev.033910

Viebahn, C. S., Benseler, V., Holz, L. E., Elsegood, C. L., Vo, M., Bertolino, P., … Yeoh, G. C. T. (2010). Invading macrophages play a major role in the liver progenitor cell response to chronic liver injury. *Journal of Hepatology*, *53*(3), 500–507. https://doi.org/10.1016/j.jhep.2010.04.010

Vladar, E. K., Antic, D., & Axelrod, J. D. (2009). Planar cell polarity signaling: the developing cell's compass. *Cold Spring Harbor Perspectives in Biology*, *1*(3), a002964. https://doi.org/10.1101/cshperspect.a002964

Wilkins, B. J., & Pack, M. (2013). Zebrafish models of human liver development and disease. *Comprehensive Physiology*, *3*(3), 1213–30. https://doi.org/10.1002/cphy.c120021

Williams, B. B., Cantrell, V. A., Mundell, N. A., Bennett, A. C., Quick, R. E., & Jessen, J. R. (2012). VANGL2 regulates membrane trafficking of MMP14 to control cell polarity and migration. *Journal of Cell Science*, *125*(9), 2141–2147. https://doi.org/10.1242/jcs.097964

Williams, B. B., Mundell, N., Dunlap, J., & Jessen, J. (2012). The planar cell polarity protein

VANGL2 coordinates remodeling of the extracellular matrix. *Communicative & Integrative Biology*, *5*(4), 325–8. https://doi.org/10.4161/cib.20291

Yin, H., Copley, C. O., Goodrich, L. V, & Deans, M. R. (2012). Comparison of phenotypes between different vangl2 mutants demonstrates dominant effects of the Looptail mutation during hair cell development. *PloS One*, *7*(2), e31988. https://doi.org/10.1371/journal.pone.0031988

Zallen, J. a. (2007). Planar polarity and tissue morphogenesis. *Cell*, *129*(6), 1051–63. https://doi.org/10.1016/j.cell.2007.05.050